


FULL PAPER

Discovery of novel furo[2,3-*d*]pyrimidin-2-one–1,3,4-oxadiazole hybrid derivatives as dual antiviral and anticancer agents that induce apoptosis

Az-eddine El Mansouri^{1,2} | Ali Oubella³ | Karim Dânoun⁴ | Mehdi Ahmad⁵ | Johan Neyts⁶ | Dirk Jochmans⁶ | Robert Snoeck⁶ | Graciela Andrei⁷ | Hamid Morjani⁷ | Mohamed Zahouily² | Hassan B. Lazrek¹ 

¹Laboratory of Biomolecular and Medicinal Chemistry, Chemistry Department, Faculty of Science Semlalia, University Cadi Ayyad, Marrakesh, Morocco

²Laboratoire de Matériaux, Catalyse & Valorisation des Ressources Naturelles, URAC 24, Département de chimie, Faculté des Sciences et Techniques, Université Hassan II, Casablanca, Morocco

³Laboratoire de Synthèse Organique et de Physico-Chimie Moléculaire, Département de Chimie, Faculté des Sciences Semlalia, Marrakech, Morocco

⁴MASCIR Foundation, Rabat Design, Rue Mohamed El Jazouli, Madinat El Irfane, 10100 Rabat, Morocco, Rabat, Morocco

⁵ICGM, Université Montpellier, CNRS, ENSCM, Montpellier, France

⁶Rega Institute for Medical Research, KU Leuven, Leuven, Belgium

⁷BioSpecT—EA7506, UFR de Pharmacie, Reims, France

Correspondence

Hassan B. Lazrek, Laboratory of Biomolecular and Medicinal Chemistry, Chemistry Department, Faculty of Science Semlalia, University Cadi Ayyad, 40000 Marrakesh, Morocco.
Email: hblazrek50@gmail.com

Abstract

A new series of furo[2,3-*d*]pyrimidine–1,3,4-oxadiazole hybrid derivatives were synthesized via an environmentally friendly, multistep synthetic tool and a one-pot Songoashira-heterocyclization protocol using, for the first time, nanostructured palladium pyrophosphate (Na₂PdP₂O₇) as a heterogeneous catalyst. Compounds **9a–c** exhibited broad-spectrum activity with low micromolar EC₅₀ values toward wild and mutant varicella-zoster virus (VZV) strains. Compound **9b** was up to threefold more potent than the reference drug acyclovir against thymidine kinase-deficient VZV strains. Importantly, derivative **9b** was not cytostatic at the maximum tested concentration (CC₅₀ > 100 μM) and had an acceptable selectivity index value of up to 7.8. Moreover, all synthesized 1,3,4-oxadiazole hybrids were evaluated for their cytotoxic activity in four human cancer cell lines: fibrosarcoma (HT-1080), breast (MCF-7 and MDA-MB-231), and lung carcinoma (A549). Data showed that compound **8f** exhibits moderate cytotoxicity, with IC₅₀ values ranging from 13.89 to 19.43 μM. Besides, compound **8f** induced apoptosis through caspase 3/7 activation, cell death independently of the mitochondrial pathway, and cell cycle arrest in the S phase for HT1080 cells and the G1/M phase for A549 cells. Finally, the molecular docking study confirmed that the anticancer activity of the synthesized compounds is mediated by the activation of caspase 3.

KEYWORDS

1,3,4-oxadiazole, anticancer, antiviral, apoptosis, furopyrimidine, heterogeneous catalyst, hybrid molecules, molecular docking

1 | INTRODUCTION

The treatment of cancer and viral diseases remains one of the major challenges to modern medicine. Cancer is the second most common cause of death after heart disease, and one in eight deaths in the world is due to cancer.^[1] On the contrary, virus infections consist of one of the primary health problems. For instance, varicella-zoster

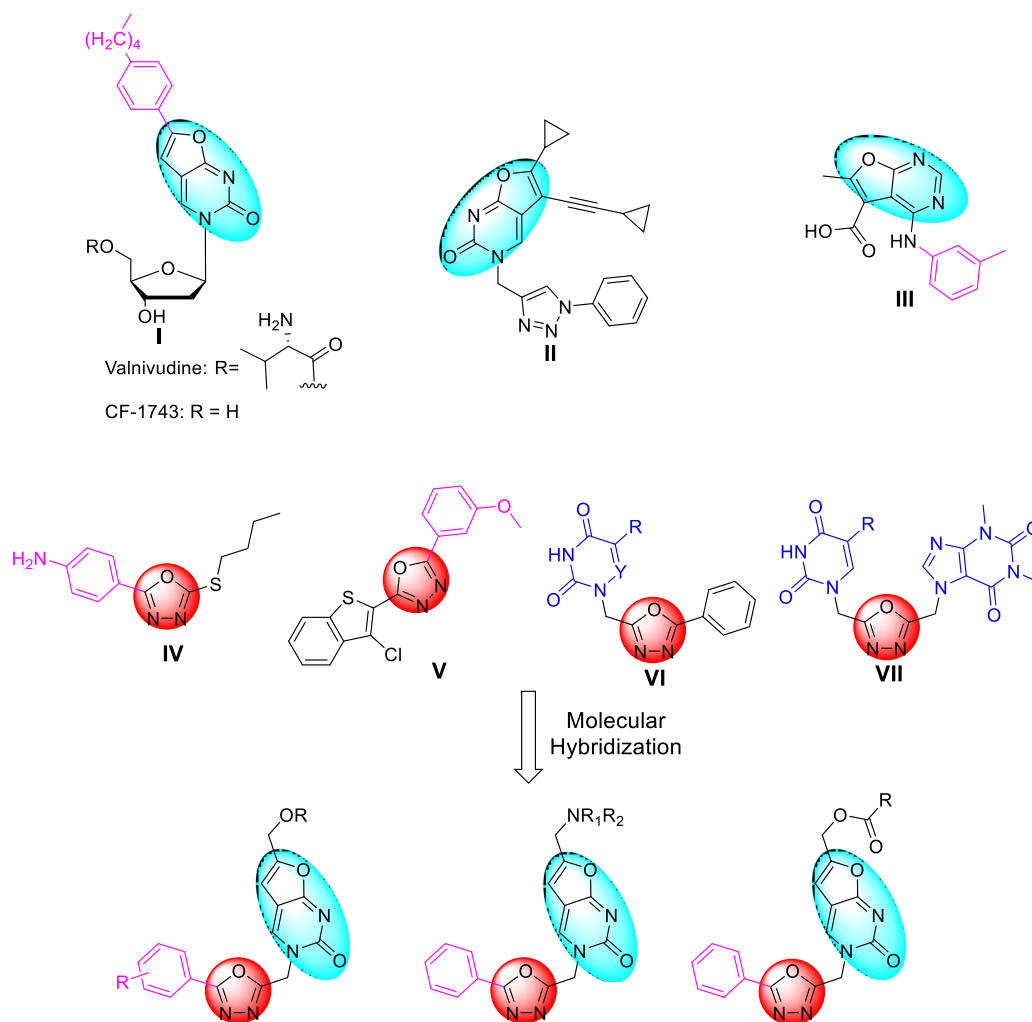
virus (VZV) infections can be life-threatening and can lead to significant morbidity and mortality for immunocompromised individuals, such as cancer patients.^[2,3] Indeed, the discovery of new anticancer and antiviral compounds remains a vital element in chemotherapy because of undesirable effects, drug resistance, and reduced bioavailability of the currently available therapeutics.^[4] Apoptosis (programmed cell death) is a fundamental biological

process that allows killing and removal of tumor cells and infected cells with pathogens.^[5] This process is mediated by the sequential activation of a family of cysteinyl–aspartate-specific proteases (caspases).^[6] Among these, caspases 3 and 7 are the crucial effector enzymes in the execution of apoptosis.^[7] Therefore, apoptosis becomes one of the attractive targets for developing new anticancer agents.^[8] Similarly, apoptotic induction of virally infected cells is an antiviral mechanism to eliminate the viruses.^[9] Brazeau and coworkers demonstrated that the death of VZV-infected human melanoma (MeWo) cells appears to be caused by apoptosis, accompanied by the activation of the caspase cascade.^[10] Moreover, immune system stimulation due to HIV infection can be the cause of apoptosis in CD4 and CD8 T-immune cells.^[11]

Pyrimidine derivatives play an essential role in antiviral and anticancer therapy, being among the first chemotherapeutic agents used in the medical treatment of cancer diseases and viral infections.^[12–14] Furo[2,3-*d*]pyrimidines were obtained by coupling a pyrimidine ring with a furan heterocycle. Bicyclic furo[2,3-*d*]pyrimidine nucleosides were developed for the first time by McGuigan et al.^[15] as herpesvirus inhibitors.

The compounds with the sugar 2'-deoxyribose are nontoxic and highly effective inhibitors of the VZV,^[16] and analogs bearing di-deoxyribose or acyclic fragments inhibited human cytomegalovirus.^[17] Moreover, a bicyclic nucleoside analog (CF-1743 I, Figure 1) has high antiviral activity against the VZV with EC₅₀ below 1 nM.^[18] Valnivadine (FV-100 free base), a prodrug of CF-1743 I, is an orally active antiherpes zoster (HZ) nucleoside analog and is rapidly and extensively converted into CF-1743 in vivo.^[19] Meanwhile, the substitution of sugar 2'-deoxyribose by methyl-1,2,3-triazole leads to improved anticancer activities. Indeed, Gregorić et al.^[20] reported that furo[2,3-*d*]pyrimidine-2-one-1,2,3-triazole hybrid **II** exhibited promising cytostatic properties against hepatocellular carcinoma (HepG2) and cervical carcinoma cells, with higher potency than the reference drug 5-fluorouracil. Also, Hossam et al.^[21] have shown that compound **III** exhibited antitumor activity comparable to that of gefitinib. This effect could be mediated at least partly via activation of apoptosis and product **III** increases the level of caspase 3 by more than twofold.^[21]

1,3,4-Oxadiazole is another widely used pharmacophore in medicinal chemistry due to its broad spectrum of biological activities.



This heterocycle is used in the treatment of viral infections (raltegravir)^[22] and cancer diseases (zibotentan).^[23] Furthermore, several 1,3,4-oxadiazole derivatives were reported to show apoptotic effects, including the activation of caspase enzymes. Sankhe et al. have synthesized compound **IV** (Figure 1), which induces apoptosis through the activation of caspase 3.^[24] A series of 1,3,4-oxadiazoles were investigated for their anticancer potential against HCC cells, and product **V** was identified as the lead compound, which induced apoptosis by the activation of caspase 3/7.^[25]

In our previous work,^[26,27] a series of 1,3,4-oxadiazole-pyrimidine hybrids (**VI**, **VII**) were synthesized and some compounds exhibited anticancer and anti-VZV activities. In continuation of our research work and based on the importance of furopyrimidines and 1,3,4-oxadiazole, we used the pharmacophore hybridization method (with the capacity to overcome resistance, enhance selectivity, and improve biological activities).^[28] Besides, we also considered the following points: (a) By introducing a furo-fused heterocycle; (b) introducing a chlorine atom into the phenyl group; (c) by improving the lipophilicity of alcohol by esterification; and (d) adding a pharmacophore group such as ibuprofen or phenol, a new series of furo[2,3-*d*]pyrimidine-2-one-1,3,4-oxadiazole hybrid analogs are synthesized. Also, we describe a synthetic methodology for the construction of furo[2,3-*d*]pyrimidine-2-one through the one-pot Sonogashira-heterocyclization method using, for the first time, nanostructured pyrophosphate palladium $\text{Na}_2\text{PdP}_2\text{O}_7$ as a highly efficient heterogeneous catalyst. Moreover, the prepared compounds were evaluated for their in vitro antiviral and selective activities against VZV, cytomegalovirus (CMV), yellow fever (YFV), chikungunya (CHIKV), human Immunodeficiency (HIV-1 and HIV-2), and human enterovirus (EV), as well as anticancer activities in HT-1080, A-549, MCF-7, and MDA-MB-231 cell lines. The most effective compound was evaluated for its effects on annexin V, mitochondrial membrane potential, caspase 3/7, and cell cycle. Finally, molecular docking was used to study the interactions of these compounds with caspase-3 protein.

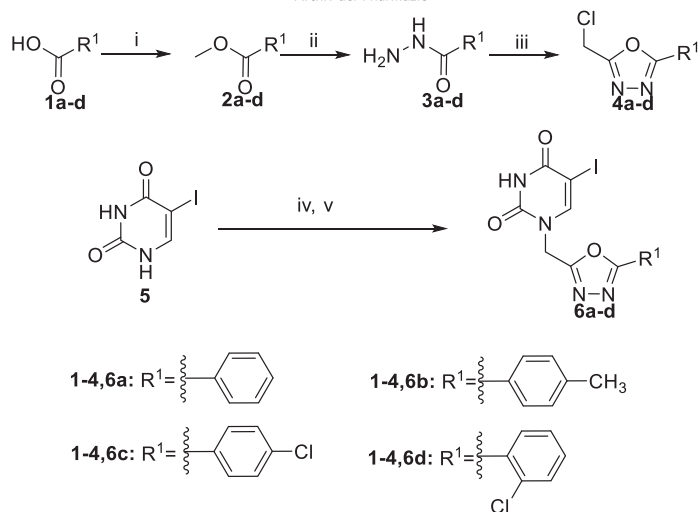
2 | RESULTS AND DISCUSSION

2.1 | Chemistry

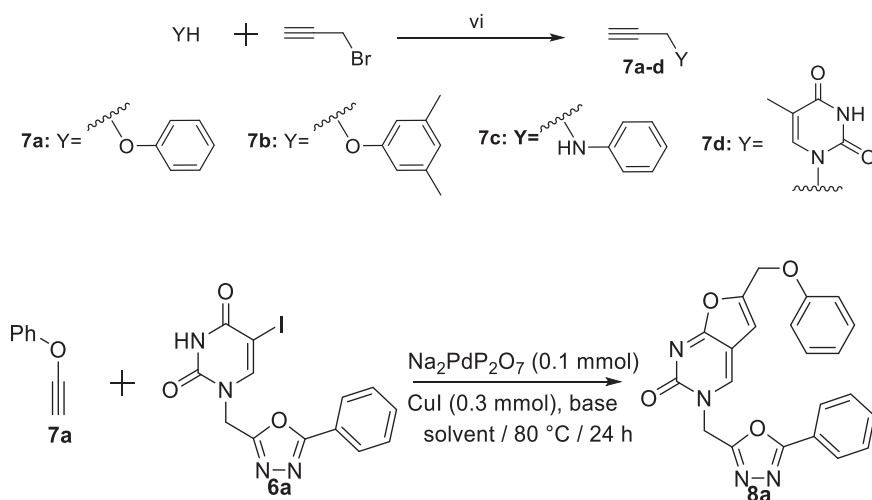
Considering the biological importance of furopyrimidine derivatives, the need for the development of an efficient synthetic methodology persists. Therefore, Sonogashira-palladium-catalyzed coupling of 5-halide uracil derivatives and alkynes, followed by intramolecular cyclization, is the most common method to access a wide variety of furo[2,3-*d*]pyrimidine derivatives.^[29,30] This process is one of the most important, powerful, and versatile methods in modern synthetic organic chemistry for constructing carbon-carbon bonds.^[29,31] The development of a one-pot reaction makes the process economic by avoiding an additional purification step (without the isolation of the intermediate alkyne).^[32] Indeed, the most heterogeneous catalyst used in this reaction is Pd

$(\text{PPh}_3)_4$ ^[20,33–37]; other catalysts were described in the literature such as $\text{PdCl}_2(\text{PPh}_3)_2$,^[38] $\text{Na}_2\text{PdCl}_4/\text{TXPTS}$,^[39] and $\text{Pd}(\text{dppf})\text{Cl}_2$.^[40] However, the described methods suffer from several limitations, including the use of air- and moisture-sensitive catalytic systems (phosphines), difficulty in the separation of palladium from the reaction, and the use of toxic reagents and ligands.^[41] On the contrary, metal pyrophosphates (MP_2O_7) have attracted considerable attention due to their attractive properties in a wide range of applications such as catalytic systems.^[42] However, only a few studies have been reported in the literature describing the use of palladium phosphate as a catalyst.^[43] For instance, our group reported that nanostructured palladium pyrophosphate ($\text{Na}_2\text{PdP}_2\text{O}_7$) exhibited high catalytic activity in Suzuki-Miyaura cross-coupling.^[44] To the best of our knowledge, the use of nanostructured pyrophosphate palladium as a heterogeneous catalyst for the preparation of furo[2,3-*d*]pyrimidines through the Sonogashira coupling reaction has not been reported in the literature.

In the present work, we described a new free ligand-catalyzed method for the preparation of furopyrimidine using a heterogeneous palladium catalyst, which is easy to separate from the reaction medium (Schemes 1–4). Indeed, we developed an environmentally friendly and multistep synthetic tool to directly obtain a new series of furo[2,3-*d*]pyrimidine-2-one-1,3,4-oxadiazole hybrid derivatives. The preparation of furo[2,3-*d*]pyrimidines is described through the one-pot Sonogashira-cyclization synthesis using $\text{Na}_2\text{PdP}_2\text{O}_7$ as a heterogeneous catalyst. To synthesize the desired products, we adopted the following strategy: the esterification of benzoic acid derivatives **1a,b** using methanol and SOCl_2 afforded the esters **2a,b**. The latter reacted with hydrazine in ethanol to give hydrazides **3a–d**. Then, the mixture of chloroacetic acid, products **3a–d** and phosphorus oxychloride (POCl_3) afforded oxadiazoles **4a–d**.^[26] After that, these chemicals were used as alkylating agents to react with iodouracil (**5**) to prepare 1,3,4-oxadiazole-pyrimidin-2,4-dione hybrids **6a–d** via the modified Hilbert-Johnson reaction.^[45] The 1,3,4-oxadiazole homonucleoside analogs were obtained in 29–35% of the yield. On the contrary, compounds **7a–d** were obtained over the alkylation reaction of amine or alcohol derivatives by propargyl bromide in a basic medium (K_2CO_3). Later, furopyrimidines were prepared from 5-iodouracils **6a–d** and propargylated products **7a–f** via a $\text{Na}_2\text{PdP}_2\text{O}_7$ -catalyzed cross-coupling reaction. The optimal conditions were investigated by changing the solvent, base, and their amount. It has been found that the use of acetonitrile/*t*-BuOH and three equivalents of triethanolamine gave the desired product with an improved yield of 56% (Entry 8, Table 1). These conditions were generalized on the reaction of 5-iodouracils **6a–d** with propargyl derivatives **7a–d** to obtain furo[2,3-*d*]pyrimidine-2-one-1,3,4-oxadiazole analogs **8a–h** in the yield ranging from 47% to 81%. Finally, to increase the lipophilicity of furopyrimidine **8a**, the esterification was performed using the activating agent dicyclohexylcarbodiimide (DCC) and different carboxylic acids including benzoic acid, amino acid boc-L-valine, and ibuprofen to afford esters **9a–c** in moderate yields. The choice of these pharmacophore groups was based on the following reasons: (i) Derivatives of benzoic acid



SCHEME 1 Synthesis of compounds **4a-d**, **6a-d**, and **7a-d**. Reagents and conditions: (i) SOCl_2 , MeOH, reflux, 6 h, (ii) NH_2NH_2 , EtOH, reflux, 3 h, (iii) $\text{ClCH}_2\text{CO}_2\text{H}$, POCl_3 , DCE, 12 h, (iv) HMDS, $(\text{NH}_4)_2\text{SO}_4$, 120°C , 3 h, (v) **4a-d**, KI, 80°C , 12 h, and (vi) K_2CO_3 , acetone, reflux, 12 h



SCHEME 2 Preparation of furopyrimidine **8a**

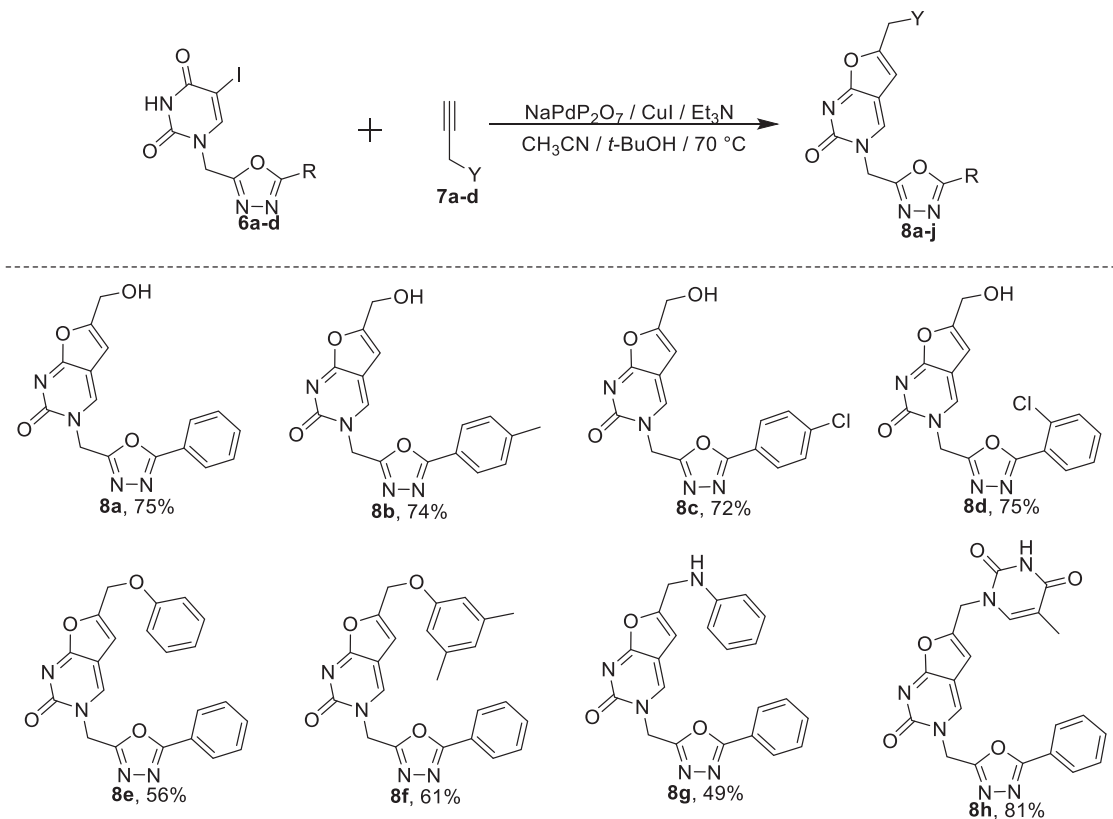
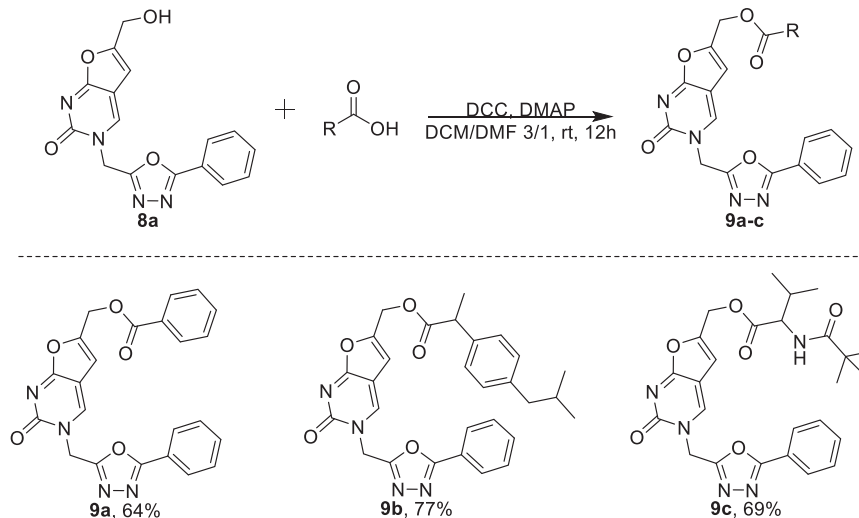
are considered as a class of simple aromatic acids known for their pharmacological properties,^[46] (ii) amino acids are widely used for the development of prodrugs to improve several properties, namely, increased bioavailability, decreased toxicity of the parent drug, accurate delivery to target tissues or organs, and prevention of fast metabolism,^[47] and (iii) ibuprofen is a widely used drug and has many applications such as for the treatment of viral respiratory infections.^[48]

2.2 | Pharmacology/biology

2.2.1 | In vitro antiviral activity

All the new molecules **8a-h** and **9a-c** were tested for their antiviral activities against the human VZV, both wild-type (TK+) and thymidine kinase-deficient (TK-), in human embryonic lung (HEL) cells. Compounds **9a-c** were the most potent and the other molecules did not show measurable activity against VZV. The growth inhibition of HEL cells was only studied for the compounds that exhibited an antiviral activity lower than $20\ \mu\text{M}$. The antiviral activities of furo

[2,3-*d*]pyrimidin-2-one-1,3,4-oxadiazole analogs (**9a-c**) were lower than that of reference drug acyclovir (ACV) against the TK+ VZV strain and they were better than that of ACV against the TK- VZV strain. Remarkably, compound **9b** was up to threefold more potent than the reference drug against TK- VZV strains. Importantly, **9b** has lower cytotoxicity ($\text{CC}_{50} > 100\ \mu\text{M}$) and an acceptable selectivity index value of up to 7.8 in comparison to acyclovir. Indeed, the product **9a** containing the benzoic acid moiety was about twofold more potent than compound **9c** (acyclic acid) against the TK+ VZV strain. Also, compound **9b** containing the ibuprofen pharmacophore group was more active than product **9c** against the TK- VZV strain. We observed that the acid-containing phenyl group increased the anti-VZV activity. Thus, the introduction of a substituted phenyl group may improve the antiviral properties. By comparing compound **8a** with molecules **9a-c**, the protection of the OH with the acyl group increased the antiviral activity. This fact is explained by the high lipophilicity of the protected compounds **9a-c**. However, lipophilicity is an essential feature of molecules in the pharmaceutical, biochemical, and medical chemistry fields.^[49] This feature is a physicochemical parameter that controls the affinity of a molecule for binding sites and the transport through biological membranes.^[50,51]

**SCHEME 3** Generalization of the reaction**SCHEME 4** Esterification reaction of furopyrimidine **8a**

In general, biological potency is often accompanied by increased molecular lipophilicity.^[52] Lipophilicity represented by the octanol/water partition coefficients (ClogP) and the products with high ClogP are more lipophilic. In this study, partition coefficients were predicted using ChemDraw. As reported in Table 2, the introduction of the acyl group increases the lipophilicity of furopyrimidines. One possible explanation for the low activity of **8a** is the cell permeability due to the low lipophilicity.

All compounds were also tested against several other viruses such as human cytomegalovirus (HCMV) (AD-169 and Davis strain) in human embryonic lung (HEL cells), yellow fever (YFV-17D strain) (HEL cells), chikungunya (CHIKV-899 strain) (VeroE6 cells), human immunodeficiency (HIV-1 IIIb strain HIV-2 ROD) (MT-4 cells), and human enterovirus 71 (EV-71 BrCr strain) (Vero cells). All tested compounds had EC_{50} higher than $100\text{ }\mu\text{M}$, except compound **9a**, which was active against the Davis strain with EC_{50} equal $54.69\text{ }\mu\text{M}$.

Entry	Solvent	Base	Equiv of base	Yield (%)
1	toluene	DIPEA	3	20
2	acetonitrile	DIPEA	3	38
3	acetonitrile/water (3/1)	DIPEA	3	12
4	acetonitrile/MeOH (3/1)	DIPEA	3	46
5	acetonitrile/PrOH (3/1)	DIPEA	3	48
6	acetonitrile/t-BuOH (3/1)	DIPEA	3	53
7	acetonitrile/t-BuOH (3/1)	K ₂ CO ₃	3	no reaction
8	acetonitrile/t-BuOH (3/1)	TEA	3	56
9	acetonitrile/t-BuOH (3/1)	TEA	1.5	32

Note: Optimal conditions: Acetonitrile/t-BuOH 3:1 (10 ml), TEA (3 equiv), Na₂PdP₂O₇ (0.1 equiv), Cul (0.3 equiv), 80°C, and 12 h.

Abbreviations: DIPEA, *N,N*-diisopropylethylamine; TEA, triethanolamine.

TABLE 1 Optimization of the preparation of furopyrimidine **8a**

TABLE 2 Antiviral and selectivity activity against the varicella-zoster virus (VZV) in human embryonic lung cells

Compound	Antiviral activity EC ₅₀ (μM) ^a		Cytotoxicity (μM)		Selectivity Index ^d		ClogP
	TK+ VZV strain	TK- VZV strain	Cell morphology (MCC) ^b	Cell growth (CC ₅₀) ^c	TK+ VZV strain	TK- VZV strain	
	OKA	07-1			CC ₅₀ /EC ₅₀		
8a	>100	>100	>100	ND	ND	ND	-1.333
9a	14.67 ± 2.21	18.34 ± 10.255	>100	44.42 ± 1.07	3.03	2.44	1.502
9b	18.18 ± 1.82	12.82 ± 0.19	>100	>100	>5.52	>7.8	3.416
9c	25.4 ± 13.7	18.08 ± 6.38	>100	46.66 ± 1.84	1.83	2.58	0.96
Acyclovir	2.48 ± 1.06	41.69 ± 3.24	>440	>440	>177.41	>10.55	-

Abbreviations: ND, not determined; OKA, Oka strain; TK+, thymidine kinase wild-type; TK-, thymidine kinase-deficient.

^aEffective concentration required to reduce virus plaque formation by 50%. Virus input was 20 plaque-forming units.

^bMinimum cytotoxic concentration that causes a microscopically detectable alteration of cell morphology.

^cCytostatic concentration required to reduce cell growth by 50%.

^dRatio: CC₅₀/EC₅₀.

Product	HT-1080	A-549	MCF-7	MDA-MB-231
8a	19.17 ± 0.21	23.60 ± 0.56	22.22 ± 0.32	26.30 ± 1.05
8b	46.31 ± 1.86	28.93 ± 0.83	37.19 ± 1.30	34.11 ± 0.92
8c	34.94 ± 1.43	36.76 ± 1.89	>100	29.34 ± 0.13
8d	35.54 ± 2.54	75.41 ± 5.81	55.03 ± 3.25	>100
8e	19.03 ± 0.68	21.28 ± 2.52	20.31 ± 3.09	25.45 ± 0.90
8f	13.89 ± 0.22	15.98 ± 0.18	19.43 ± 0.48	17.32 ± 1.07
8g	18.98 ± 0.63	21.03 ± 3.11	28.09 ± 2.85	18.54 ± 1.45
8h	17.21 ± 1.48	27.19 ± 3.90	37.39 ± 4.52	33.21 ± 1.03
9a	18.33 ± 2.51	23.34 ± 1.27	50.34 ± 6.46	28.02 ± 0.34
9b	19.39 ± 1.21	28.44 ± 0.88	35.98 ± 1.16	39.02 ± 1.72
9c	29.21 ± 2.82	36.01 ± 3.09	35.60 ± 3.88	32.77 ± 2.60
Doxorubicin	6.36 ± 0.38	4.96 ± 0.07	5.46 ± 0.44	5.13 ± 0.31

TABLE 3 In vitro anticancer activity (IC₅₀) of 1,3,4-oxadiazole hybrids (**8a-i** and **9a-c**) against HT1080, A549, MCF7, and MDA-MB231 cells

2.2.2 | In vitro anticancer screening

All the newly synthesized products were evaluated for their cytotoxicity in human HT-1080, A-549, MCF-7, and MDA-MB-23 cell lines with doxorubicin as the positive control using the MTT assay. The antiproliferative activities of the furopyrimidine-1,3,4-oxadiazole hybrid derivatives are shown in Table 3. First, the structure-activity relationship study focused on the variation of substituted phenyl at the 5-attachment of 1,3,4-oxadiazole. The substitution of hydrogen in phenyl by a methyl group (**8b**) at the *para* or chlorine atom at *ortho* and *para* positions (**8c–d**) decreased the anticancer potency. Then, we retained the nonsubstituted phenyl moiety (**8a**) and we have replaced OH at position 6 of the furopyrimidine base with an aniline group to give compound **8g**, which showed moderately decreased activity in all human cancer cell lines, whereas product **8h**, possessing a thymine nucleobase at the same position, exhibited less anticancer activity in comparison to compound **8a**. Next, the OH had different carboxyl functions to afford compounds **9a–c**; product **9a** has the same antiproliferative activity as furopyrimidine **8a** against HT-1080 and A-549. Finally, the replacement of the hydrogen atom of OH with phenyl (**8e**, ether bound) and 3,5-dimethylphenyl (**8f**) increased the anticancer activity in all cell lines. In summary, the hybrid furopyrimidine

(**8f**) with the phenyl moiety at the 5-position of the 1,3,4-oxadiazole heterocycle and dimethylphenoxymethyl at the 6-position of the furopyrimidine base was the most potent, with IC₅₀ values of 13.89 ± 0.22 , 15.98 ± 0.18 , 19.43 ± 0.48 , and $17.32 \pm 1.07 \mu\text{M}$ against HT-1080, A-549, MCF-7, and MDA-MB-23, respectively.

2.2.3 | Annexin V/7-AAD staining to detect apoptosis

The most potent compound **8f** was tested for its apoptotic induction activity using flow cytometric annexin V/7-AAD dual staining analysis. The HT-1080 and A-549 cancer cell lines were treated with $15 \mu\text{M}$ of the most potent compound **8f** for 24 h to study the apoptosis-dependent cell death. The results (Figure 2) showed an increase in total apoptosis in HT-1080 by about 21-fold (from 1.28% to 26.47%) compared to the control untreated cancer cells. Individually, early and late apoptosis increased by approximately 6-fold and 43-fold, respectively. Also, compound **8f** induced apoptosis in A-549 by ninefold from 1.76% to 15.71% (early apoptosis 1.47–4.31% and late apoptosis 0.29–11.4%). In conclusion, hybrid derivative **8f** showed the ability to induce apoptosis-dependent cell death in HT-1080 and A-549 cancer cell lines.

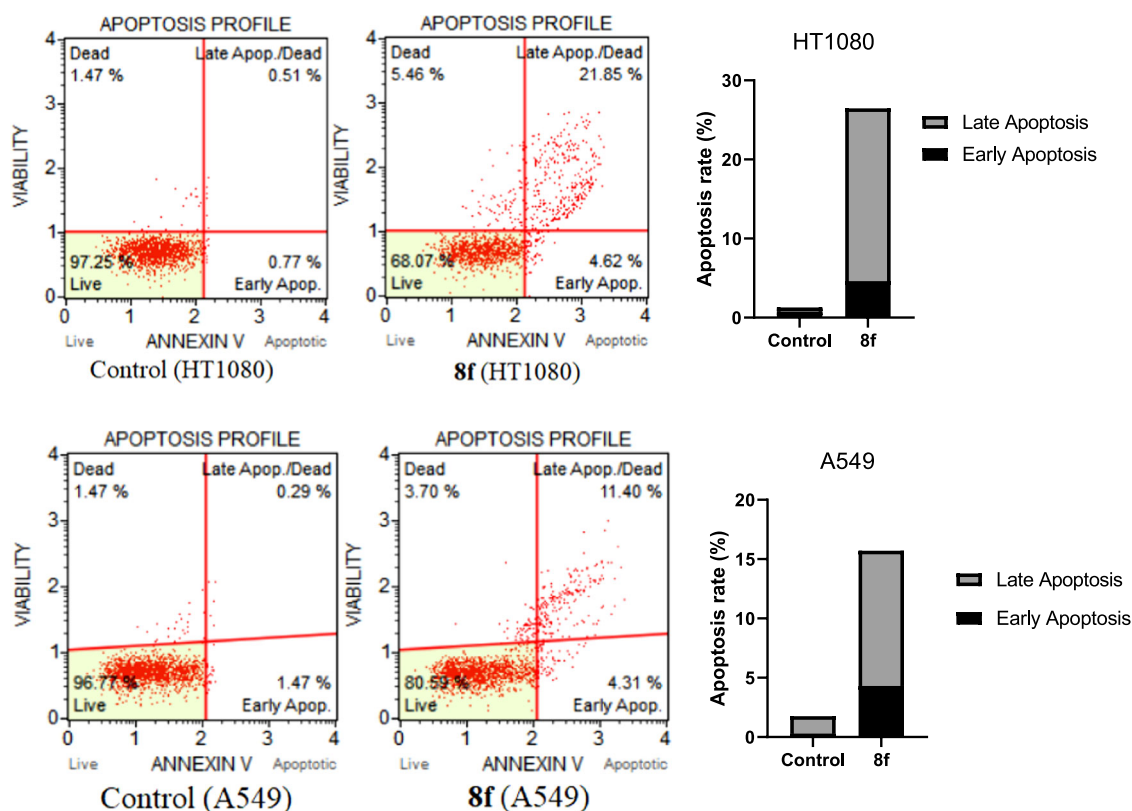


FIGURE 2 Annexin V-FITC/7-AAD double staining for detection of apoptosis in HT-1080 and A-549 cells after treatment with $15 \mu\text{M}$ of compound **8f** as well as control (dimethyl sulfoxide) for 24 h. Compound **8f** induces apoptosis

2.2.4 | Effect of compound **8f** on the mitochondrial membrane potential (MMP)

The dysfunction of MMP was also reported to involve induction of apoptosis. In this study, mitochondrial dysfunction was determined based on the MMP index that was measured by flow cytometry using the Muse MitoPotential Kit (Millipore-Merck). HT-1080 and A-549 cells were treated with compound **8f** at 15 μ M concentration for 24 h. As shown in Figure 3, compound **8f** induced an increase in the MMP index. In fact, in the case of HT-1080 cells, the rate of dead cells with high MMP increased from 5.605% \pm 1.963% to 20.03% \pm 0.064%. Similarly, in A-549 cells, this rate increased from 5.840% \pm 1.501% to 19.51% \pm 1.5%. This suggests that compound **8f** can induce cell death independently of the mitochondrial pathway.

2.2.5 | Effect of compound **8f** on caspase-3/-7 activity

The mechanism of apoptosis induction by the most active product **8f** in HT-1080 and A-549 was investigated by the determination of caspase-3/-7 percentages. The cells were treated with 15 μ M of compound **8f** for 24 h; all the results are summarized in Figure 4. In the HT-1080 cancer cell, furoprymidine **8f** increased the percentage of caspase 3/7 by about fourfold from 7.185% \pm 0.72% to 29.44% \pm 0.42% in comparison to the control. Similarly, the product **8f** also induced caspase 3/7 by increasing its percentage from

7.81% \pm 0.38% to 13.685% \pm 2.51%. In summary, these data are in agreement with those obtained on annexin V staining and suggest that the product **8f** induced apoptosis through caspase 3/7 in both cells, especially in the HT-1080 cancer line.

2.2.6 | Effect of compound **8f** on cell cycle distribution

Flow cytometry was used to explore the effects of compound **8f** on cell cycle progression. HT-1080 and A-549 cells were treated with 15 μ M of the compound for 24 h. As shown in Figure 5, the treatment of HT-1080 cells with compound **8f** increased cell cycle arrest in the S phase, resulting in an increase in the cell population in the S phase (10.25% \pm 0.05%) compared to the control cells (13.3% \pm 0.1%). Moreover, treatment of A-549 cells with compound **8f** increased cell cycle arrest in the G1M phase from 11.57% \pm 0.15% to 15.8% \pm 0.2% compared to the untreated cells. These results demonstrate that in HT-1080 and A-549 cells, cell cycle arrest occurs in the S and G1M phases, which contributes to the cytotoxicity of the compound **8f**.

2.3 | Molecular docking

With the aim of continuing the investigation of apoptosis induction mechanism via the caspase activation, in silico molecular docking was studied. Also, taking into account the docking study of oxadiazole

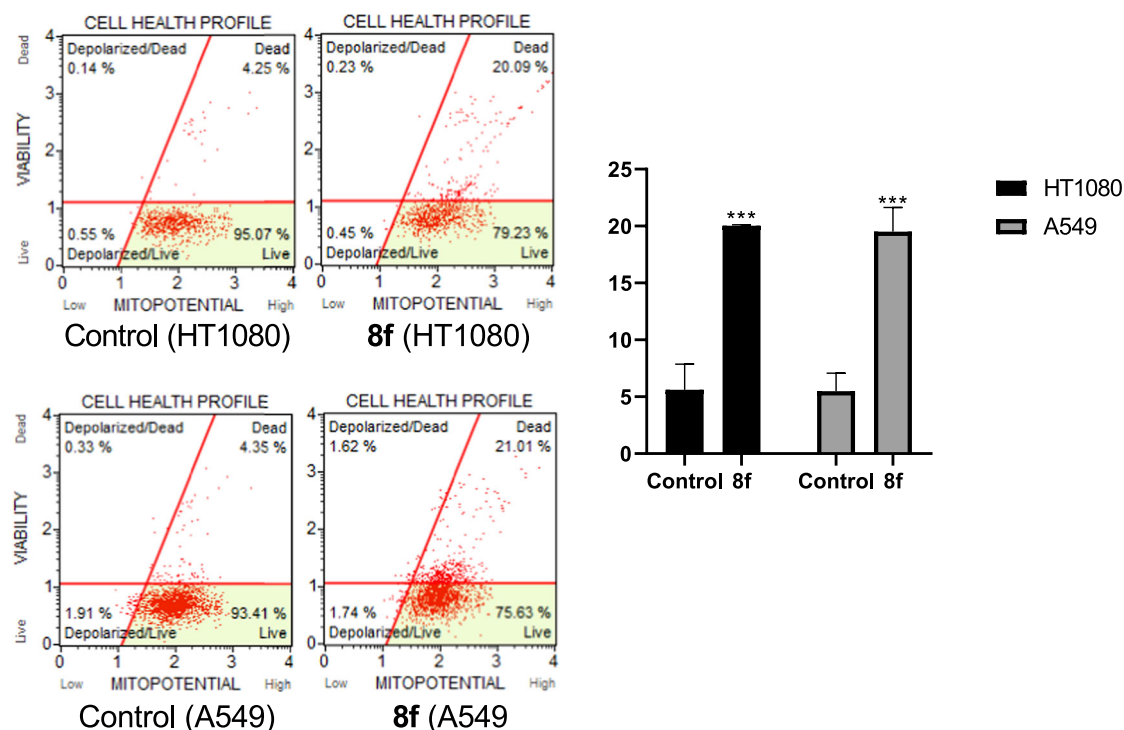


FIGURE 3 Flow cytometric analysis (FACS) of the mitochondrial membrane potential in HT-1080 and A-549 cells treated with compound **8f** at 15 μ M concentration for 24 h (data represent mean \pm SD of three individual experiments)

FIGURE 4 Induction of caspase 3/7 activity in response to compound **8f**. HT-1080 and A-549 cells were treated with 15 μ M of the desired compound as well as dimethyl sulfoxide (control) for 24 h (data represent mean \pm SD of three individual experiments)

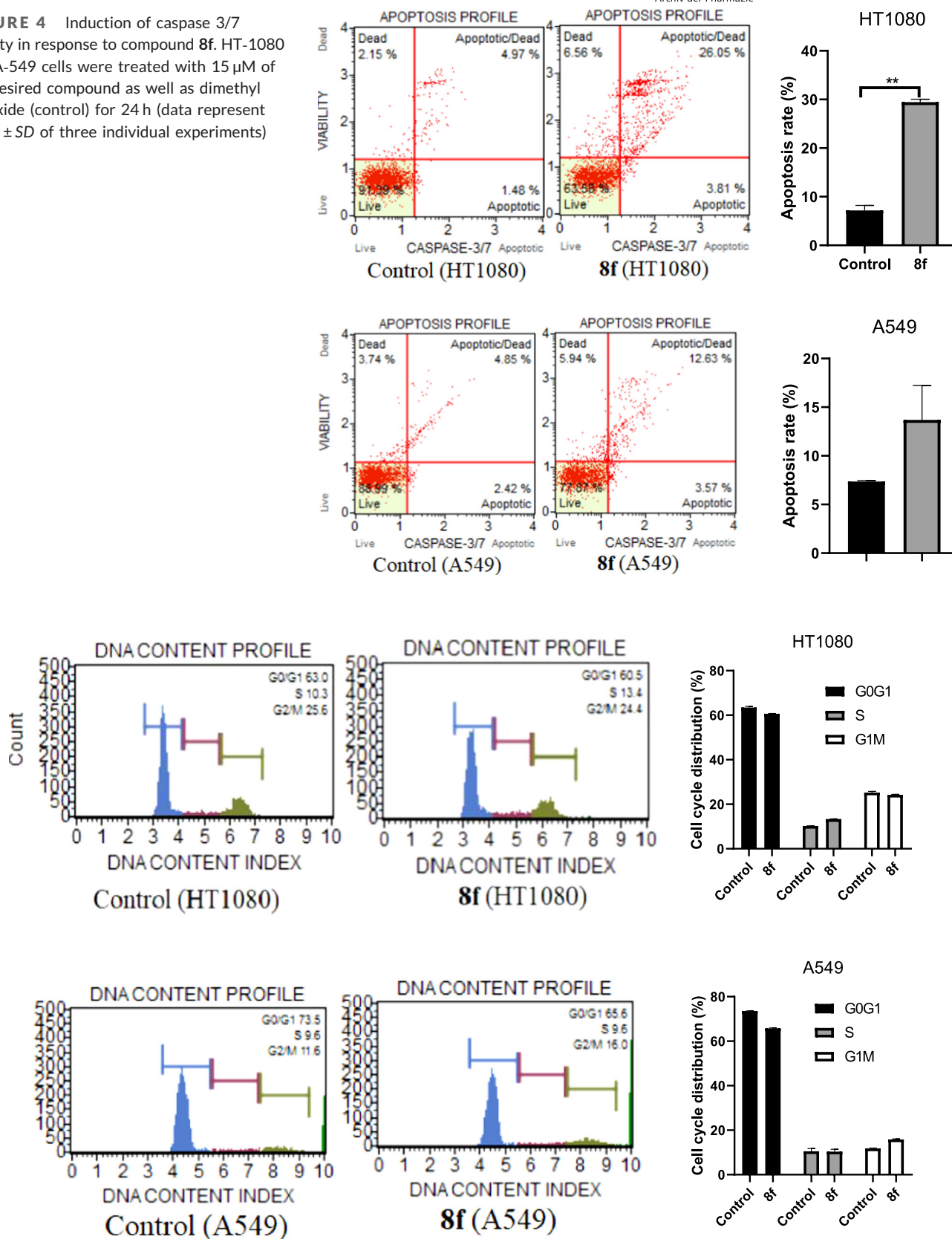


FIGURE 5 Flow cytometry analysis of cell cycle phase distribution in HT-1080 and A-549 cells after treatment of 15 μ M of compound **8f** in comparison with the control for 24 h. Compound **8f** induced S-phase arrest for HT1080 and G1M arrest for A549 cells (data represent mean \pm SD of three individual experiments)

derivatives as potent caspase-3 activators,^[27,53,54] compound **8f** was selected and docked into the binding site of caspase 3 (PDB ID: 1RE1). Before this, to determine the validity of our docking protocol, self-docking experiments were carried out. The root-mean-square deviations between the predicted and the native poses were found to be 0.95 Å. These results indicated that the adopted docking protocol is good for the reproduction of the native poses (<2 Å).

The docking results of the oxadiazole **8f** with caspase 3 are summarized in Figures 6–8 and in the Supporting Information Table. Compound **8f** could be docked into the active site of caspase 3 with the estimated free energy of binding -10.4 kcal/mol. The docked pose of **8f** was surrounded by a partially hydrophobic cavity, especially the phenyl and dimethylphenyl moieties (Figure 6). This ligand formed six H bonds with the amino acid residues ARG179 (2.534 Å), ARG179 (2.306 Å), HIS237 (1.827 Å), GLN283 (2.034 Å), ARG341 (2.368 Å), and ARG341 (2.477 Å). Also, other interactions were observed, such as a carbon–hydrogen bond, π -cation, π -donor hydrogen bond, π -sulfur, π - π T-shaped, and π -alkyl. This result is in agreement with the literature, in which it has been reported that these binding interactions are fundamental for caspase 3 activation.^[27,54–57] In summary, the binding affinities and the interactions were in good agreement with apoptosis induction via caspase activation. The ligands showed heterogeneity in binding modes, including H-bond interactions. Besides, the promising activity of compound **8f** could be mediated by binding to active sites of caspase 3.

3 | CONCLUSIONS

In conclusion, a new free ligand-catalyzed method for the preparation of furopyrimidine using heterogeneous pyrophosphate palladium $\text{Na}_2\text{PdP}_2\text{O}_7$ has been reported. A novel series of furo[2,3-*d*]pyrimidine-2-one-1,3,4-oxadiazole hybrid derivatives were synthesized for the first time as antiviral and anticancer agents. Furopyrimidine **9b** was up to threefold more potent than the reference drug against TK- VZV and was not cytostatic at the maximum tested concentration ($\text{CC}_{50} > 100 \mu\text{M}$). Besides, among the synthesized derivatives, **8f** showed the best cytotoxic activity against four human

cancer cell lines HT-1080, A-549, MCF-7, and MDA-MB-23. The mechanism of the antiproliferative effect on HT-1080 and A-549 was proapoptotic through activation of caspase 3/7, cell death independently of the mitochondrial pathway, and cell arrest in the S phase for HT1080 and the G1M phase for A-549. Finally, molecular docking showed that compound **8f** entered deep into the active site of caspase 3 by forming stable complexes (H-bond, carbon–hydrogen bond, etc.). These results suggested that the anticancer activity of the product **8f** could be at least partially mediated by binding to caspase 3.

4 | EXPERIMENTAL

4.1 | Chemistry

4.1.1 | General

Melting points were measured using a Büchi B-545 digital capillary melting point apparatus and used without correction. Reactions were checked with thin-layer chromatography (TLC) using aluminum sheets with silica gel 60 F254 from Merck. Infrared (IR) spectra were recorded on a Perkin-Elmer VERTEX 70 FTIR spectrometer covering field $400\text{--}4000 \text{ cm}^{-1}$. The spectra of ^1H NMR (nuclear magnetic resonance) and ^{13}C NMR (see the Supporting Information) were recorded in solution in $\text{DMSO-}d_6$ or CDCl_3 on a Bruker Advance 300 spectrometer at 300 and 75 MHz, respectively. The chemical shifts are expressed in parts per million (ppm) using $\text{DMSO-}d_6$ as the internal reference. The multiplicities of the signals are indicated by the following abbreviations: s, singlet; d, doublet; t, triplet; q, quadruplet; and m, multiplet. Coupling constants J are expressed in Hertz. Mass spectra were collected using an API 3200 LC/MS/MS system, equipped with an ESI source. The chemical reagents used in synthesis were purchased from Fluka, Sigma, and Aldrich.

The InChI codes of the investigated compounds, together with some biological activity data, are provided in the Supporting Information.

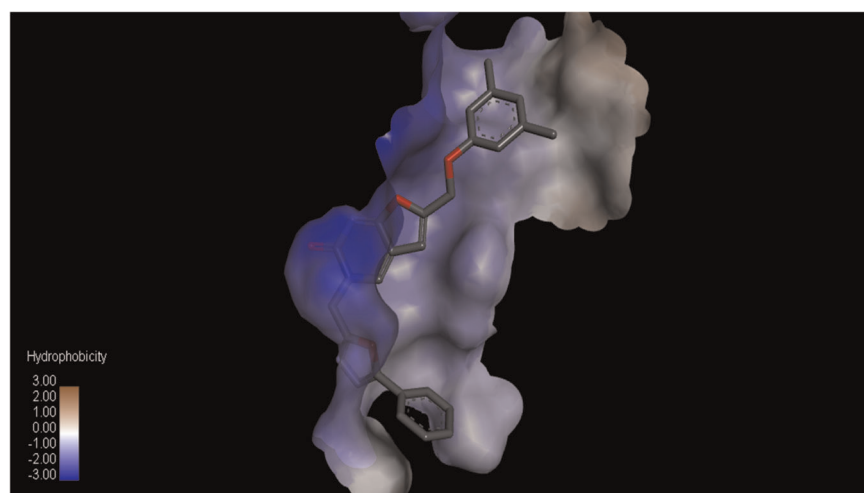


FIGURE 6 Position of ligand **8f** in the hydrophobic cavity of caspase 3

FIGURE 7 Three-dimensional interactions of compound **8f** with the amino acid residues of caspase 3

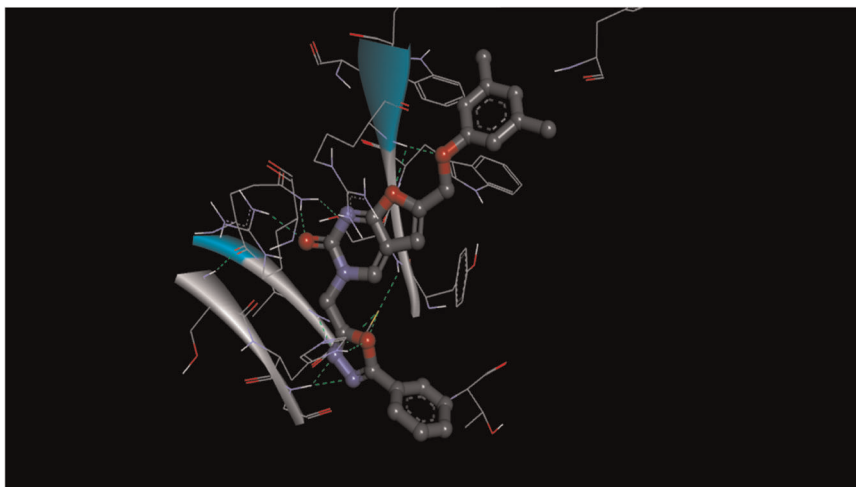
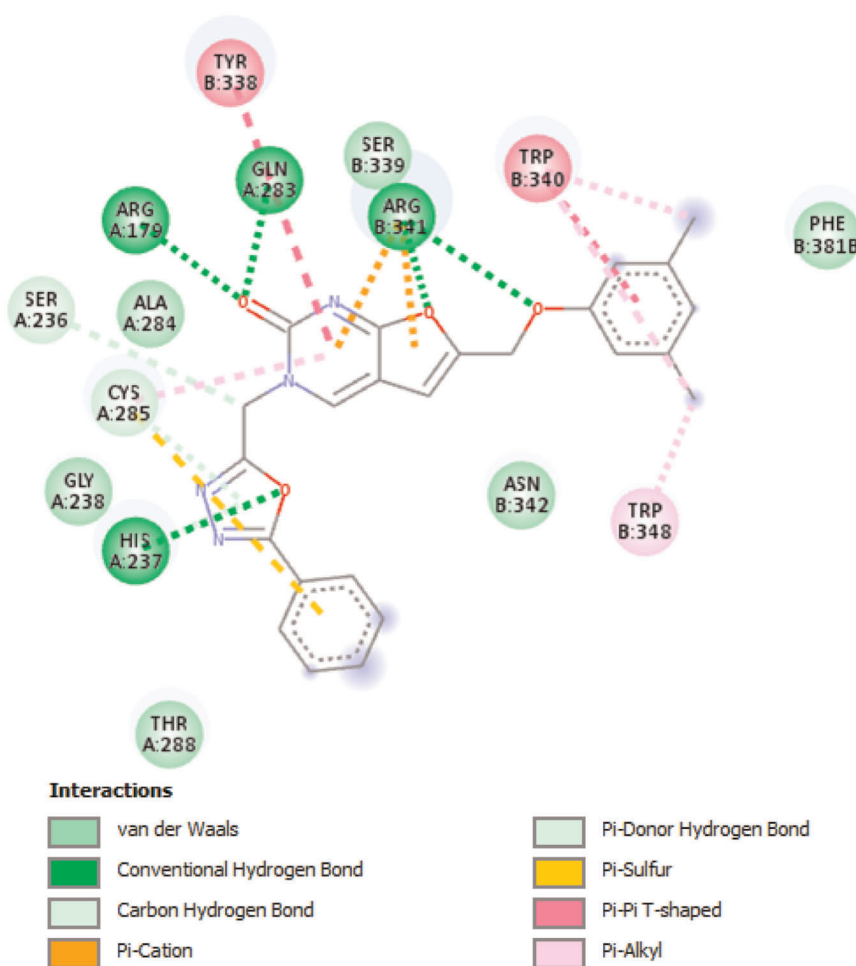


FIGURE 8 Two-dimensional interactions of compound **8f** with the amino acid residues of caspase 3



4.1.2 | General procedure for the synthesis of alkylating agents **4a-d**

First, 10 mmol carboxylic acid **1a-d** was taken in 15 ml of methanol, and thionyl chloride was added dropwise for 10 min at 0°C. Then, the mixture was stirred at room temperature for 3 h and methanol was evaporated under vacuum, extracted with ethyl acetate, and

purified by column chromatography to afford esters **2a-d**. In the second step, to a round-bottom flask (25 ml) equipped with a condenser, a mixture of esters **2a-d** (10 mmol), hydrazine hydrate (11 mmol, 0.5 ml), and ethanol (5 ml) was added. The mixture was refluxed for 3 h. The solvent was evaporated under vacuum and the hydrazide was recrystallized using ethanol to afford the desired products **3a-d**. Then, chloroacetic acid (11 mmol, 1.04 g),

phosphorus oxychloride (30 mmol, 2.8 ml), and DCE (20 ml) were mixed in a 100 ml round-bottom flask and heated at 80°C for 2 h. Afterward, carboxylic acid hydrazide (**3a–d**) was added to the mixture and heated for 12 h. After completion of the reaction, water (40 ml) was added and the pH was adjusted to 7–8 with sodium hydrogen carbonate and extracted with dichloromethane. The organic layer was dried (Na₂SO₄), evaporated, and purified by column chromatography (silica gel, 5% EtOAc in hexane) to give the alkylating agents **4a–d**.

2-(Chloromethyl)-5-phenyl-1,3,4-oxadiazole (**4a**)

Yield = 68%. R_f = 0.4 (9:1 [hexane/AcOEt]). Mp (°C) 105–107. IR (KBr) ν (cm⁻¹): 3029 (Csp²H), 2972 (Csp³H), 1552 (C=N), 1017 (C–O–C), and 746 (C–Cl). ¹H NMR (300 MHz, CDCl₃) δ (ppm): 5.16 (s, 2H, H-1); 7.6 (m, 3H, H_{Ph}); 8.03 (m, 2H, H_{Ph}). ¹³C NMR (75 MHz, CDCl₃) δ (ppm): 33.23 (C-1); 122.85 (C_{Ph, IV}); 126.65 (C_{Ph, III}); 129.53 (C_{Ph, III}); 132.38 (C_{Ph, III}); 162.88, 164.95 (C-2, C-3).

2-(Chloromethyl)-5-(4-methylphenyl)-1,3,4-oxadiazole (**4b**)

Yield = 75%. R_f = 0.46 (9:1 [hexane/AcOEt]). Mp (°C) 112–114. IR (KBr) ν (cm⁻¹): 3020 (Csp²H), 2965 (Csp³H), 1562 (C=N), 1018 (C–O–C), and 760 (C–Cl). ¹H NMR (300 MHz, CDCl₃) δ (ppm): 2.49 (s, 3H, H-4); 5.58 (s, 2H, H-1); 7.39 (d, ³J_{H-H} = 8.1 Hz, 2H, H_{Ph}); 7.82 (d, ³J_{H-H} = 8.1 Hz, 2H, H_{Ph}). ¹³C NMR (75 MHz, CDCl₃) δ (ppm): 21.64 (C-4); 39.12 (C-1); 115.04 (C_{Ph, IV}); 126.87 (C_{Ph, III}); 130.50 (C_{Ph, III}); 132.85 (C_{Ph, IV}); 162.81, 164.77 (C-2, C-3).

2-(Chloromethyl)-5-(4-chlorophenyl)-1,3,4-oxadiazole (**4c**)

Yield = 68%. R_f = 0.34 (9:1 [hexane/AcOEt]). Mp (°C) 83–85. IR (KBr) ν (cm⁻¹): 3021 (Csp²H), 2964 (Csp³H), 1568 (C=N), 1011 (C–O–C), and 756 (C–Cl). ¹H NMR (300 MHz, CDCl₃) δ (ppm): 5.15 (s, 2H, H-1); 7.66 (t, ³J_{H-H} = 7.5 Hz, 2H, H_{Ph}); 8.01 (d, ³J_{H-H} = 7.5 Hz, 2H, H_{Ph}). ¹³C NMR (75 MHz, CDCl₃) δ (ppm): 36.23 (C-1); 121.09 (C_{Ph, IV}); 124.62 (C_{Ph, III}); 125.37 (C_{Ph, III}); 136.45 (C_{Ph, IV}); 162.28, 164.12 (C-2, C-3).

2-(Chloromethyl)-5-(2-chlorophenyl)-1,3,4-oxadiazole (**4d**)

Yield = 70%. R_f = 0.35 (9:1 [hexane/AcOEt]). Mp (°C) 91–93. IR (KBr) ν (cm⁻¹): 3018 (Csp²H), 2964 (Csp³H), 1554 (C=N), 1013 (C–O–C), and 753 (C–Cl). ¹H NMR (300 MHz, CDCl₃) δ (ppm): 5.22 (s, 2H, H-1); 7.5 (t, ³J_{H-H} = 7.6 Hz, 1H, H_{Ph}); 7.62 (d, ³J_{H-H} = 7.2 Hz, 1H, H_{Ph}); 7.69 (t, ³J_{H-H} = 7.2 Hz, 1H, H_{Ph}); 7.93 (t, ³J_{H-H} = 7.6 Hz, 1H, H_{Ph}). ¹³C NMR (75 MHz, CDCl₃) δ (ppm): 35.41 (C-1); 122.65 (C_{Ph, IV}); 127.82 (C_{Ph, III}); 131.52 (C_{Ph, III}); 131.83 (C_{Ph, III}); 132.37 (C_{Ph, III}); 133.98 (C_{Ph, IV}); 162.35, 164.22 (C-2, C-3).

4.1.3 | General procedure for the synthesis of the alkylated 5-iodouracil derivatives **6a–d**

A mixture of 5-iodouracil **5** (1 mmol, 238 mg) and ammonium sulfate (0.10 mmol, 13 mg) in HMDS (1.5 ml) was refluxed until a clear solution was obtained. Then, the appropriate alkylating agent **4a–d**

(1.5 mmol), KI (0.75 mmol, 124 mg), and acetonitrile (2.5 ml) were added. The reaction mixture was heated at 85°C for 12 h. After completion of the reaction (monitored by TLC), the mixture was diluted with dichloromethane and evaporated to dryness. The residue was purified by flash chromatography by eluting with (CH₂Cl₂/MeOH: 99:1).

5-Iodo-1-[(5-phenyl-1,3,4-oxadiazol-2-yl)methyl]pyrimidine-2,4(1H,3H)-dione (**6a**)

Yield = 35%. R_f = 0.42 (CH₂Cl₂/CH₃OH [9.6:0.4]). Mp (°C) 282–284. IR (KBr) ν (cm⁻¹): 1707 (C=O), 1614 (C=N), 1554 (C=C), and 1246 (C–O–C). ¹H NMR (300 MHz, DMSO-*d*₆) δ (ppm): 5.3 (s, 2H, H-7); 7.64 (m, 3H, H_{Ph}); 8 (m, 2H, H_{Ph}); 8.38 (s, 1H, H-6); 11.85 (s, 1H, H-3). ¹³C NMR (75 MHz, DMSO-*d*₆) δ (ppm): 42 (C-7); 70 (C-5); 123 (C_{Ph, IV}); 126 (C_{Ph, IV}); 129 (C_{Ph, IV}); 133 (C_{Ph, IV}); 150 (C-6); 151 (C-2); 161 (C-4); 162, 164 (C-8, C-9).

5-Iodo-1-[[5-(p-tolyl)-1,3,4-oxadiazol-2-yl]methyl]pyrimidine-2,4(1H,3H)-dione (**6b**)

Yield = 35%. R_f = 0.45 (CH₂Cl₂/CH₃OH [9.6:0.4]). Mp (°C) 289–291. IR (KBr) ν (cm⁻¹): 1706 (C=O), 1619 (C=N), 1548 (C=C), and 1242 (C–O–C). ¹H NMR (300 MHz, DMSO-*d*₆) δ (ppm): 2.42 (s, 1H, H-10); 5.38 (s, 2H, H-7); 7.33 (d, ³J_{H-H} = 7.8 Hz, 2H, H_{Ph}); 7.97 (d, ³J_{H-H} = 7.8 Hz, 2H, H_{Ph}); 8.24 (1H, s, H-6); 11.72 (1H, s, H-3). ¹³C NMR (75 MHz, DMSO-*d*₆) δ (ppm): 21.18 (C-10); 45.36 (C-7); 71.39 (C-5); 115.54 (C_{Ph, IV}); 126.35 (C_{Ph, III}); 130.62 (C_{Ph, III}); 132.83 (C_{Ph, IV}); 150.14 (C-6); 150.96 (C-2); 161.93 (C-4); 162.30, 164.91 (C-8, C-9).

1-[[5-(4-Chlorophenyl)-1,3,4-oxadiazol-2-yl]methyl]-5-iodopyrimidine-2,4(1H,3H)-dione (**6c**)

Yield = 32%. R_f = 0.41 (CH₂Cl₂/CH₃OH [9.6:0.4]). Mp (°C) 290–292. IR (KBr) ν (cm⁻¹): 1704 (C=O), 1618 (C=N), 1541 (C=C), and 1239 (C–O–C). ¹H NMR (300 MHz, DMSO-*d*₆) δ (ppm): 5.12 (s, 2H, H-7); 7.25 (d, ³J_{H-H} = 8 Hz, 2H, H_{Ph}); 8.04 (d, ³J_{H-H} = 8 Hz, 2H, H_{Ph}); 8.31 (1H, s, H-6); 11.69 (1H, s, H-3). ¹³C NMR (75 MHz, DMSO-*d*₆) δ (ppm): 44.86 (C-7); 71.43 (C-5); 116.11 (C_{Ph, IV}); 126.80 (C_{Ph, III}); 130.14 (C_{Ph, III}); 133.25 (C_{Ph, IV}); 150.07 (C-6); 151.48 (C-2); 162.36 (C-4); 162.87, 165.35 (C-8, C-9).

1-[[5-(2-Chlorophenyl)-1,3,4-oxadiazol-2-yl]methyl]-5-iodopyrimidine-2,4(1H,3H)-dione (**6d**)

Yield = 29%. R_f = 0.42 (CH₂Cl₂/CH₃OH [9.6:0.4]). Mp (°C) 289–291. IR (KBr) ν (cm⁻¹): 1704 (C=O), 1614 (C=N), 1542 (C=C), and 1231 (C–O–C). ¹H NMR (300 MHz, DMSO-*d*₆) δ (ppm): 5.20 (s, 2H, H-7); 7.38 (t, ³J_{H-H} = 7.6 Hz, 1H, H_{Ph}); 7.52 (d, ³J_{H-H} = 7.5 Hz, 1H, H_{Ph}); 7.78 (t, ³J_{H-H} = 7.6 Hz, 1H, H_{Ph}); 8.04 (t, ³J_{H-H} = 8 Hz, 1H, H_{Ph}); 8.29 (1H, s, H-6); 11.71 (1H, s, H-3). ¹³C NMR (75 MHz, DMSO-*d*₆) δ (ppm): 45.25 (C-7); 72.89 (C-5); 121.74 (C_{Ph, IV}); 127.33 (C_{Ph, III}); 131.81 (C_{Ph, III}); 132.05 (C_{Ph, III}); 132.20 (C_{Ph, III}); 133.63 (C_{Ph, IV}); 150.41 (C-6); 151.96 (C-2); 162.29 (C-4); 163.27, 165.56 (C-8, C-9).

4.1.4 | General procedure for the synthesis of the propargylated derivatives **7a-d**

A mixture of phenol or amine derivative (1 mmol), propargyl bromide (1.1 mmol), and potassium carbonate (0.5 mmol, 69 mg) in DMF (10 ml) was heated at 90°C for 2 h. Then, the DMF was evaporated under reduced pressure to dryness. The residue was purified by flash chromatography to obtain pure product **7a-d**.

4.1.5 | General procedure for the synthesis of furo [2,3-d]pyrimidin-2(3H)-ones **8a-h**

The appropriate 5-iodouracil analog **6a-d** (0.4 mmol), propargylated derivative **7a-d** (1.2 mmol), CuI (0.12 mmol, 23 mg), and Na₂PdP₂O₇ (0.04 mmol, 13 mg) were dissolved in CH₃CN/t-BuOH: 3/1 (4 ml). The *N,N*-diisopropylethylamine (3.6 mmol, 0.6 ml) was added slowly at 0°C, and then the mixture was stirred at 70°C for 12 h. The solvent was evaporated under reduced pressure and the residue was purified using column chromatography (CH₂Cl₂-MeOH) to obtain pure products **8a-h**.

3-[[5-(5-Phenyl-1,3,4-oxadiazol-2-yl)methyl]-6-(hydroxymethyl)furo[2,3-d]pyrimidin-2(3H)-one (**8a**)

Yield = 75%. R_f = 0.32 (CH₂Cl₂/MeOH [9:1]). Mp (°C): 186–187. IR (KBr) ν (cm⁻¹): 3339 (OH), 3051 (Csp²H), 2847 (Csp³H), 1687 (C=O), 1611 (C=N), 1240 (C–O–C). R_f = 0.32 (CH₂Cl₂/MeOH [9:1]). ¹H NMR (300 MHz, DMSO-*d*₆) δ (ppm): 4.52 (d, ³J_{H-H} = 6 Hz, 2H, CH₂-O); 5.49 (s, 2H, CH₂-N); 5.63 (t, ³J_{H-H} = 6 Hz, 1H, OH); 6.67 (s, 1H, H-5); 7.48 (m, 3H, H_{ph}); 8.04 (d, ³J_{H-H} = 8 Hz, 2H, H_{ph}); 8.79 (s, 1H, H-4). ¹³C NMR (75 MHz, DMSO-*d*₆) δ (ppm): 46.03 (CH₂-N); 56.31 (CH₂-O); 104.30 (C-5); 107.38 (C-4a); 123.19 (C_{ph,IV}); 127.36 (C_{ph,III}); 129.02 (C_{ph,III}); 132.27 (C_{ph,III}); 143.83 (C-4); 154.92 (C-2); 158.46 (C-7a); 162.92 (O–C=N); 165.21 (O–C=N); 172.77 (C-6). HRMS calculated for C₁₆H₁₃N₄O₄⁺: 325.0937, found 325.0947.

6-(Hydroxymethyl)-3-[[5-(*p*-tolyl)-1,3,4-oxadiazol-2-yl)methyl]furo[2,3-d]pyrimidin-2(3H)-one (**8b**)

Yield = 74%. R_f = 0.36 (CH₂Cl₂/MeOH [9:1]). Mp (°C): 218–220. IR (KBr) ν (cm⁻¹): 3387 (OH), 3033 (Csp²H), 2964 (Csp³H), 1675 (C=O), 1621 (C=N), and 1162 (C–O–C). ¹H NMR (300 MHz, DMSO-*d*₆) δ (ppm): 2.38 (s, 3H, CH₃); 4.46 (d, ³J_{H-H} = 5.7 Hz, 2H, CH₂-O); 5.52 (s, 2H, CH₂-N); 5.81 (t, ³J_{H-H} = 5.7 Hz, 1H, OH); 6.68 (s, 1H, H-5); 7.39 (d, ³J_{H-H} = 8.1 Hz, 2H, H_{ph}); 7.85 (d, ³J_{H-H} = 8.1 Hz, 2H, H_{ph}); 8.72 (s, 1H, H-4). ¹³C NMR (75 MHz, DMSO-*d*₆) δ (ppm): 21.69 (CH₃); 46.01 (CH₂-N); 56.38 (CH₂-O); 101.37 (C-5); 107.36 (C-4a); 120.85 (C_{ph,IV}); 127.08 (C_{ph,III}); 130.60 (C_{ph,III}); 142.93 (C_{ph,IV}); 143.88 (C-4); 154.92 (C-2); 158.45 (C-7a); 162.89 (O–C=N); 165.02 (O–C=N); 172.70 (C-6). HRMS calculated for C₁₇H₁₅N₄O₄⁺: 339.1088, found: 339.1105.

3-[[5-(4-Chlorophenyl)-1,3,4-oxadiazol-2-yl)methyl]-6-(hydroxymethyl)furo[2,3-d]pyrimidin-2(3H)-one (**8c**)

Yield = 72%. R_f = 0.34 (CH₂Cl₂/MeOH [9:1]). Mp (°C): 230–232. IR (KBr) ν (cm⁻¹): 3079 (Csp²H), 2941 (Csp³H), 1686 (C=O), 1575

(C=N), and 1228 (C–O–C). ¹H NMR (300 MHz, DMSO-*d*₆) δ (ppm): 4.45 (d, ³J_{H-H} = 5.7 Hz, 2H, CH₂-O); 5.53 (s, 2H, CH₂-N); 5.61 (t, ³J_{H-H} = 5.7 Hz, 1H, OH); 6.68 (s, 1H, H-5); 7.66 (d, ³J_{H-H} = 8.4 Hz, 2H, H_{ph}); 7.97 (d, ³J_{H-H} = 8.4 Hz, 2H, H_{ph}); 8.72 (s, 1H, H-4). ¹³C NMR (75 MHz, DMSO-*d*₆) δ (ppm): 46.00 (CH₂-N); 56.36 (CH₂-O); 101.38 (C-5); 107.38 (C-4a); 122.44 (C_{ph,IV}); 128.93 (C_{ph,III}); 130.24 (C_{ph,III}); 137.48 (C_{ph,IV}); 143.89 (C-4); 154.93 (C-2); 158.46 (C-7a); 163.34 (O–C=N); 164.17 (O–C=N); 172.70 (C-6). HRMS calculated for C₁₆H₁₂ClN₄O₄⁺: 359.0547, found: 359.0557.

3-[[5-(2-Chlorophenyl)-1,3,4-oxadiazol-2-yl)methyl]-6-(hydroxymethyl)furo[2,3-d]pyrimidin-2(3H)-one (**8d**)

Yield = 75%. R_f = 0.35 (CH₂Cl₂/MeOH [9:1]). Mp (°C): 176–178. IR (KBr) ν (cm⁻¹): 3438 (OH), 3051 (Csp²H), 2847 (Csp³H), 1687 (C=O), 1611 (C=N), and 1165 (C–O–C). ¹H NMR (300 MHz, DMSO-*d*₆) δ (ppm): 4.45 (d, ³J_{H-H} = 6 Hz, 2H, CH₂-O); 5.55 (s, 2H, CH₂-N); 5.60 (t, ³J_{H-H} = 6 Hz, 1H, OH); 6.68 (s, 1H, H-5); 7.55 (t.d, ³J_{H-H} = 7.5 Hz, ³J_{H-H} = 7.8 Hz, 1H, H_{ph}); 7.64 (t.d, ³J_{H-H} = 8.1 Hz ³J_{H-H} = 7.8 Hz, 1H, H_{ph}); 7.64 (d.d, ³J_{H-H} = 8.1 Hz ³J_{H-H} = 7.5 Hz, 1H, H_{ph}); 7.70 (d.d, ³J_{H-H} = 8.1 Hz, ³J_{H-H} = 7.8 Hz, 1H, H_{ph}); 7.93 (d.d, ³J_{H-H} = 7.8 Hz ³J_{H-H} = 8.1 Hz, 1H, H_{ph}); 8.73 (s, 1H, H-4). ¹³C NMR (75 MHz, DMSO-*d*₆) δ (ppm): 46.02 (CH₂-N); 56.36 (CH₂-O); 101.34 (C-5); 107.36 (C-4a); 122.75 (C_{ph,IV}); 128.52 (C_{ph,III}); 131.74 (C_{ph,III}); 131.84 (C_{ph,III}); 132.35 (C_{ph,IV}); 133.98 (C_{ph,III}); 143.90 (C-4); 154.92 (C-2); 158.48 (C-7a); 163.01 (O–C=N); 163.55 (O–C=N); 172.71 (C-6). C₁₆H₁₂ClN₄O₄⁺: 359.0547, found: 359.0555.

6-(Phenoxymethyl)-3-[[5-(5-phenyl-1,3,4-oxadiazol-2-yl)methyl]furo[2,3-d]pyrimidin-2(3H)-one (**8e**)

Yield = 59%. R_f = 0.56 (CH₂Cl₂/MeOH [9.5:0.5]). Mp (°C): 230–232. IR (KBr) ν (cm⁻¹): 3079 (Csp²H), 2941 (Csp³H), 1686 (C=O), 1575 (C=N), and 1228 (C–O–C). ¹H NMR (300 MHz, DMSO-*d*₆) δ (ppm): 5.16 (s, 2H, CH₂-O); 5.54 (s, 2H, CH₂-N); 6.99 (m, 4H, H-5 + 3H_{ph}); 7.31 (m, 2H, H_{ph}); 7.59 (m, 3H, H_{ph}); 7.96 (m, 2H, H_{ph}); 8.82 (s, 1H, H-4). ¹³C NMR (75 MHz, DMSO-*d*₆) δ (ppm): 45.39 (CH₂-N); 61.72 (CH₂-O); 104.51 (C-5); 106.23 (C-4a); 114.92 (C_{ph,III}); 121.31 (C_{ph,III}); 123.02 (C_{ph,IV}); 126.52 (C_{ph,III}); 129.41 (C_{ph,III}); 129.51 (C_{ph,III}); 132.08 (C_{ph,III}); 144.416 (C-4); 152.426 (C_{ph,IV}-O); 154.629 (C-2); 157.629 (C-7a); 162.414 (O–C=N); 164.341 (O–C=N); 171.98 (C-6). HRMS calculated for C₂₂H₁₇N₄O₄⁺: 401.1258, found: 401.1250.

6-[[3,5-Dimethylphenoxy)methyl]-3-[[5-(5-phenyl-1,3,4-oxadiazol-2-yl)memethyl]furo[2,3-d]pyrimidin-2(3H)-one (**8f**)

Yield = 61%. R_f = 0.59 (CH₂Cl₂/MeOH [9.5:0.5]). Mp (°C): 219–212. IR (KBr) ν (cm⁻¹): 3022 (Csp²H), 2954 (Csp³H), 1675 (C=O), 1578 (C=N), and 1157 (C–O–C). ¹H NMR (300 MHz, DMSO-*d*₆) δ (ppm): 2.83 (s, 6H, CH₃); 4.51 (s, 2H, CH₂-O); 4.96 (s, 2H, CH₂-N); 6.05 (s, 1H, H_{ph}); 6.12 (s, 2H, H_{ph}); 6.41 (s, 1H, H-5); 7.04 (m, 3H, H_{ph}); 7.4 (d, ³J_{H-H} = 7.8 Hz, 2H, H_{ph}); 8.26 (s, 1H, H-4). ¹³C NMR (75 MHz, DMSO-*d*₆) δ (ppm): 20.99 (CH₃); 45.50 (CH₂-N); 61.47 (CH₂-O); 104.44 (C-5); 106.36 (C-4a); 112.51 (C_{ph,III}); 122.91 (C_{ph,III}); 123.15 (C_{ph,IV}); 126.54 (C_{ph,III}); 129.48 (C_{ph,III}); 132.18 (C_{ph,III}); 138.76 (C_{ph,IV}); 144.51 (C-4); 152.58 (C-2); 157.58 (C-7a); 162.48 (O–C=N); 164.37

(O=C=N); 172.09 (C-6). HRMS calculated for $C_{24}H_{21}N_4O_4^+$: 429.1563, found: 429.1571.

3-[(5-Phenyl-1,3,4-oxadiazol-2-yl)methyl]-6-[(phenylamino)methyl]-furo[2,3-d]pyrimidin-2(3H)-one (8g)

Yield = 49%. Rf = 0.48 ($CH_2Cl_2/MeOH$ [9.5:0.5]). Mp (°C): 217–219. IR (KBr) ν (cm^{-1}): 3432 (NH), 3040 (Csp2H), 2844 (Csp3H), 1685 (C=O), 1571 (C=N), and 1163 (C–O–C). 1H NMR (300 MHz, DMSO- d_6) δ (ppm): 3.90 (d, $^3J_{H-H} = 6$ Hz, 2H, CH_2 -NH); 5.06 (s, 2H, CH_2 -N); 5.79 (t, $^3J_{H-H} = 6$ Hz, 1H, NH); 6.12 (t, $^3J_{H-H} = 7.2$ Hz, 1H, H_{Ph}); 6.20 (s, 1H, H-5); 6.23 (d, $^3J_{H-H} = 7.8$ Hz, 2H, H_{Ph}); 6.63 (t, $^3J_{H-H} = 7.5$ Hz, 2H, H_{Ph}); 7.158 (m, 3H, H_{Ph}); 7.510 (dd, $^3J_{H-H} = 7.2$ Hz $^3J_{H-H} = 8.1$ Hz, 2H, H_{Ph}); 8.217 (s, 1H, H_4). ^{13}C NMR (75 MHz, DMSO- d_6) δ (ppm): 40.51 (CH_2); 45.50 (CH_2); 101.24 (C-5); 107.00 (C-4a); 112.58 ($C_{Ph, III}$); 116.62 ($C_{Ph, III}$); 123.15 ($C_{Ph, IV}$); 126.68 ($C_{Ph, III}$); 129.03 ($C_{Ph, III}$); 129.60 ($C_{Ph, III}$); 132.27 ($C_{Ph, III}$); 143.04 (C-4); 147.98 ($C_{Ph, IV-N}$); 154.41 (C-2); 156.29 (C-7a); 162.70 (O=C=N); 164.48 (O=C=N); 172.17 (C-6). HRMS calculated for $C_{22}H_{18}N_5O_3^+$: 400.1410, found: 400.1419.

5-Methyl-1-[[2-oxo-3-[(5-phenyl-1,3,4-oxadiazol-2-yl)methyl]-2,3-dihydrofuro[2,3-d]pyrimidin-6-yl]methyl]pyrimidine-2,4(1H,3H)-dione (8h)

Yield = 81%. Rf = 0.24 ($CH_2Cl_2/MeOH$ [9:1]). Mp (°C): 237–239. IR (KBr) ν (cm^{-1}): 3433 (NH), 3036 (Csp2H), 2826 (Csp3H), 1672 (C=O), 1570 (C=N), and 1176 (C–O–C). 1H NMR (DMSO- d_6 , 300 MHz) δ (ppm): 1.77 (s, 3H, CH_3); 4.93 (s, 2H, CH_2 -N); 5.54 (s, 2H, CH_2 -N); 6.81 (s, 1H, H-5); 7.61 (m, 4H, $H_{Ph} + H_6$); 7.98 (d, $^3J_{H-H} = 6.9$ Hz, 2H, H_{Ph}); 8.77 (s, 1H, H_4); 11.41 (s, 1H, NH). ^{13}C NMR (DMSO- d_6 , 75 MHz) δ (ppm): 11.93 (CH_3); 43.35 (CH_2 -N); 45.42 (CH_2 -N); 103.18 (C-5); 106.43 (C-5'); 109.35 (C-4a); 122.97 ($C_{Ph, IV}$); 126.53 ($C_{Ph, III}$); 129.45 ($C_{Ph, III}$); 132.13 ($C_{Ph, III}$); 140.56 (C-6'); 144.03 (C-4); 150.64 (C-4'); 152.01 (C-2); 154.16 (C-7a); 162.47 (O=C=N); 164.15 (O=C=N); 164.32 (C-2'); 171.88 (C-6). HRMS calculated for $C_{21}H_{17}N_6O_5^+$: 433.1260, found: 433.1267.

4.1.6 | General procedure for the synthesis of furopyrimidine esters **9a–c**

Carboxylic acid (0.2 mmol), DCC (0.22 mmol, 45 mg), and furopyrimidine **8a** (0.2 mmol, 65 mg) in dichloromethane/DMF (2:1 ml) with catalytic amounts of 4-dimethylaminopyridine (DMAP) were stirred mechanically at room temperature for 12 h. *N,N*-Dicyclohexylurea formed was filtered off. The filtrate was washed with 5% acetic acid (12 ml) and water (12 ml) and dried over anhydrous sodium sulfate. The solvent was removed under reduced pressure and the residue was chromatographed over a column of silica gel using $CH_2Cl_2/MeOH$ (99:1, v/v) as an eluent.

{2-Oxo-3-[(5-phenyl-1,3,4-oxadiazol-2-yl)methyl]-2,3-dihydrofuro[2,3-d]pyrimidin-6-yl}methyl benzoate (9a)

Yield = 64%. Rf = 0.59 ($CH_2Cl_2/MeOH$ [9.5:0.5]). Mp (°C): 145–147. IR (KBr) ν (cm^{-1}): 3034 (Csp2H), 2970 (Csp3H), 1738 (C=O), 1681 (C=O), 1568 (C=N), and 1156 (C–O–C). 1H NMR (300 MHz, $CDCl_3$) δ (ppm): 5.30 (s, 2H, CH_2 -O); 5.57 (s, 2H, CH_2 -N); 6.62 (s, 1H, H-5); 7.45 (m, 6H,

H_{Ph}); 8.02 (m, 4H, H_{Ph}); 8.27 (s, 1H, H-4). ^{13}C NMR (75 MHz, $CDCl_3$) δ (ppm): 44.59 (CH_2 -N); 58.15 (CH_2 -O); 103.98 (C-5); 107.36 (C-4a); 123.06 ($C_{Ph, IV}$); 127.14 ($C_{Ph, III}$); 128.53 ($C_{Ph, III}$); 129.13 ($C_{Ph, III}$); 129.84 ($C_{Ph, III}$); 132.25 ($C_{Ph, III}$); 133.56 ($C_{Ph, III}$); 140.86 (C-4); 150.01 ($C_{Ph, IV}$); 153.16 (C-2); 154.82 (C-7a); 162.96 (O=C=N); 164.13 (O=C=N); 165.86 (O=C=O); 172.40 (C-6). HRMS calculated for $C_{23}H_{17}N_4O_5^+$: 429.1199, found: 429.1205.

{2-Oxo-3-[(5-phenyl-1,3,4-oxadiazol-2-yl)methyl]-2,3-dihydrofuro[2,3-d]pyrimidin-6-yl}methyl 2-(4-isobutylphenyl)propanoate (9b)

Yield = 77%. Rf = 0.63 ($CH_2Cl_2/MeOH$ [9.5:0.5]). Mp (°C): 162–164. IR (KBr) ν (cm^{-1}): 3034 (Csp2H), 2970 (Csp3H), 1735 (C=O), 1672 (C=O), 1566 (C=N), and 1172 (C–O–C). 1H NMR (300 MHz, $CDCl_3$) δ (ppm): 0.88 (d, $^3J_{H-H} = 6.6$ Hz, 6H, CH_3 -CH- CH_2); 1.51 (d, $^3J_{H-H} = 7.2$ Hz, 3H, CH_3 -CH); 1.84 (s, $^3J_{H-H} = 6.6$ Hz, 1H, CH_3 -CH- CH_2); 1.84 (d, $^3J_{H-H} = 6.6$ Hz, 2H, CH_2 -CH); 3.76 (q, $^3J_{H-H} = 7.2$ Hz, 1H, CH - CH_2); 5.01 (AB-system, $^3J_{H-H} = 14$ Hz, 1H, (CH_2)_a-O); 5.08 (AB-system, $^3J_{H-H} = 14$ Hz, 1H, (CH_2)_b-O); 5.55 (s, 2H, CH_2 -N); 6.34 (s, 1H, H-5); 7.09 (d, $^3J_{H-H} = 8.1$ Hz, 2H, H_{Ph}); 7.20 (d, $^3J_{H-H} = 8.1$ Hz, 2H, H_{Ph}); 7.52 (m, 3H, H_{Ph}); 8.09 (d.d, $^3J_{H-H} = 8.4$ Hz $^3J_{H-H} = 7.8$ Hz, 2H, H_{Ph}); 8.14 (s, 1H, H-4). ^{13}C NMR (75 MHz, $CDCl_3$) δ (ppm): 18.33 (CH_3); 22.35 (CH_3); 30.14 (CH); 44.35 (CH_2); 44.90 (CH); 44.98 (CH_2); 57.94 (CH_2 -O); 103.16 (C-5); 108.08 (C-4a); 123.06 ($C_{Ph, IV}$); 127.16 ($C_{Ph, III}$); 129.13 ($C_{Ph, III}$); 129.44 ($C_{Ph, III}$); 132.27 ($C_{Ph, III}$); 136.96 ($C_{Ph, IV}$); 140.26 (C-4); 140.86 ($C_{Ph, IV}$); 153.25 (C-2); 154.75 (C-7a); 161.29 (O=C=N); 166.07 (O=C=N); 172.33 (C-6); 173.98 (O=C=O). HRMS calculated for $C_{26}H_{30}N_5O_6^+$: 508.2191, found: 508.2198.

{2-Oxo-3-[(5-phenyl-1,3,4-oxadiazol-2-yl)methyl]-2,3-dihydrofuro[2,3-d]pyrimidin-6-yl}methyl pivaloylvalinate (9c)

Yield = 69%. Rf = 0.55 ($CH_2Cl_2/MeOH$ [9.5:0.5]). Mp (°C): 168–170. IR (KBr) ν (cm^{-1}): 3031 (Csp2H), 2969 (Csp3H), 1733 (C=O), 1687 (C=O), 1565 (C=N), and 1170 (C–O–C). 1H NMR (300 MHz, $CDCl_3$) δ (ppm): 0.88 (d, $^3J_{H-H} = 6.9$ Hz, 3H, CH_3 -CH); 0.95 (d, $^3J_{H-H} = 6.9$ Hz, 3H, CH_3 -CH); 1.45 (s, 9H, CH_3 -C); 2.14 (m, 1H, CH - CH_2); 4.24 (m, 1H, CH -N); 5.07 (AB-system, $^3J_{H-H} = 13.8$ Hz, 1H, (CH_2)_a-O); 5.17 (AB-system, $^3J_{H-H} = 13.8$ Hz, 1H, (CH_2)_b-O); 5.57 (s, 2H, CH_2 -N); 6.57 (s, 1H, H-5); 7.09 (d, $^3J_{H-H} = 8.1$ Hz, 2H, H_{Ph}); 7.53 (m, 3H, H_{Ph}); 8.01 (d, $^3J_{H-H} = 8.1$ Hz, 2H, H_{Ph}); 8.25 (s, 1H, H-4). ^{13}C NMR (75 MHz, $CDCl_3$) δ (ppm): 17.61 (CH_3 -CH); 19.01 (CH_3 -CH); 28.29 (CH_3 -C); 31.10 (CH - CH_2); 44.56 (CH_2 -N); 58.11 (CH_2 -O); 58.67 (N-CH-CO); 104.04 (C-5); 107.92 (C-4a); 123.06 ($C_{Ph, IV}$); 127.12 ($C_{Ph, III}$); 129.13 ($C_{Ph, III}$); 132.26 ($C_{Ph, III}$); 141.02 (C-4); 152.54 (C-2); 154.79 (C-7a); 161.356 (O=C=N); 165.99 (O=C=N); 171.84 (C-6); 172.34 (O=C=O). HRMS calculated for $C_{29}H_{29}N_4O_5^+$: 513.2138, found: 513.2146.

4.2 | Pharmacological/biological assays

4.2.1 | Antiviral activity evaluation

The antiviral assays were based on inhibition of virus-induced cytopathic or plaque formation in HEL cells against the VZV, TK+ (Oka

strain), and TK— (07-1 strain) and against HCMV AD-169 and Davis strains. Confluent cell cultures in microtiter 96-well plates were infected with 100 (for HCMV) with 20 plate-forming units for VZV. After 2 h adsorption, the viral inoculum was removed and the cell cultures were incubated with fresh medium in the presence of varying concentrations of the test compounds. Viral plaque formation for VZV or the viral cytopathic effect (for HCMV) was recorded after, respectively, 5 and 7 days postinfection. Antiviral activity was expressed as the EC_{50} or compound concentration required to reduce the viral cytopathic effect (HCMV) or viral plaque formation (VZV) by 50%. Alternatively, the cytostatic activity of the test compounds was measured based on inhibition of cell growth. HEL cells were seeded at a rate of 5×10^3 cells/well into 96-well microtiter plates and allowed to proliferate for 24 h. Then, medium containing different concentrations of the test compounds was added. After 3 days of incubation at 37°C, the cell number was determined using a Coulter counter. The cytostatic concentration was calculated as CC_{50} , or the compound concentration required to reduce cell proliferation by 50% relative to the number of cells in the untreated controls.

4.2.2 | Anticancer activity evaluation

Cell culture

Four cancer cell lines HT-1080 fibrosarcoma, A-549 lung carcinoma, MCF-7, and MDA-MB-231 breast adenocarcinoma were kindly provided by Dr. P. Coursaget from INSERM (Tours, France). A-549, MCF-7, and MDA-MB-231 cells were cultured in Dulbecco's modified Eagle's medium, whereas HT-1080 cells were cultured in MEM (minimum essential medium) culture media, both supplemented with 10% (v/v) fetal bovine serum and 1% penicillin–streptomycin. The cells were incubated at 37°C in a humidified atmosphere with 5% CO_2 .

Antiproliferative activity

Cells were seeded in 96-well plates at a density of 5×10^3 cells/well for 24 h. Subsequently, cells were treated with various concentrations of compounds **8a–h** and **9a–c** for 24 h. Doxorubicin (TEVA Pharma S.A.) was used as a positive control. Then, cell growth was analyzed using the MTT (3[4,5-dimethylthiazol-2-yl]-2,5-diphenyl tetrazolium bromide) assay. Cells were incubated with 5 mg/ml of MTT for 4 h at +37°C. The supernatant was then discarded before dissolving the product of the reaction of formazan with 150 μ l of DMSO. The absorbance was then measured at 570 nm wavelength using a microplate reader (Thermo Fisher Scientific). IC_{50} was estimated using GraphPad Prism7.

Annexin V-binding assay

Cells were seeded at a density of 2×10^5 /well and incubated overnight at 37°C. The cells were then treated with compound **8f** at a concentration of 15 μ M for 24 h. Cells were then harvested and washed twice with phosphate-buffered saline (PBS) at 4°C. Then, the cells were centrifuged at 300g for 5 min and washed twice with PBS

at 4°C, before adding 100 μ l of annexin V-binding buffer staining (Annexin V Apoptosis Detection KIT with 7-AAD; Millipore-Merck). The cells were then incubated for 20 min at room temperature in the dark. Apoptotic cells were evaluated using a Muse Cell Analyzer (Millipore-Merck).

Mitochondrial membrane potential measurement

The Muse MitoPotential Kit was used to determine the mitochondrial membrane potential (Millipore-Merck). The cells were treated with compound **8f** at a concentration of 5 μ M. After harvesting and washing, the cells were resuspended in 5×10^5 cells/ml in the assay buffer. Then, to each 100 μ l cell suspension, 90 μ l of the MitoPotential working solution was added. After 20 min incubation at 37°C, 5 μ l of the Muse MitoPotential 7-AAD reagent was added to each sample. After 5 min incubation, cells were analyzed using the Muse flow cytometer (Millipore-Merck).

Caspase-3/-7 activity

Cells were treated with 15 μ M concentration of the compound **8f**. After 24 h incubation, cells were then harvested and washed twice with PBS at 4°C. After staining with the Caspase Assay Kit (Promega) and incubation for 30 min, caspase-3 activity was analyzed according to the manufacturer's instructions and using the Muse Cell Analyzer (Millipore-Merck).

Cell cycle assay

Cells were treated with 15 μ M of the compound **8f** for 24 h. The cells were then harvested and washed with PBS. The collected cells (10^6 cells) were suspended in 70% ice-cold ethanol at –20°C for fixation. After washing, the cells were pelleted by gentle centrifugation and suspended in 1 ml of staining buffer (100 mM Tris, pH 7.4, 150 mM NaCl, 1 mM $CaCl_2$, 0.5 mM $MgCl_2$, 0.1% Nonidet P-40) containing 3 μ M propidium iodide (Millipore-Merck). The cells were then incubated for 15 min at room temperature and analyzed for cell cycle phase distribution using the Muse Cell Analyzer (Millipore-Merck).

4.3 | Molecular docking

In silico computational docking studies were performed using AutoDock 4.2.^[58] The X-ray crystallographic structure of caspase 3 was downloaded from the RCSB Protein Data Bank (PDB) ID: 1RE1.^[59] The protein was prepared separately by removing water and cocrystallized ligands bound with the protein to make remove any ligand from the receptor free before docking. Then, polar hydrogen and Gastieger charges were added using the MGL Tools and proteins saved in PDBQT format. The ligand structure was created separately using ChemDraw Ultra 12.0, energy was minimized in Chem3D, and torsional bonds of the ligand were set to be flexible and saved in PDBQT format.^[60] Next, the receptor was kept rigid and a grid covering all the amino acid residues present inside the active site of proteins was built (grid box size

of $50 \times 50 \times 50 \text{ \AA}$ with a spacing of 0.375 \AA between the grid points and centered at 35.58 [x], 94.397 [y], and 17.54 [z]). The best conformers were searched using the Lamarckian genetic algorithm, the population size was set to 150, and the maximum number of energy evaluations was set to 25,000,000. Finally, the results were analyzed and visualized using Discovery Studio.

ACKNOWLEDGMENTS

The authors would like to thank the technical staff of the University of Montpellier, Montpellier, France, the University Cadi Ayyad Marrakech, and Faculty of Sciences and Technologies Mohammedia, University Hassan II Casablanca, Morocco, for running the spectroscopic analysis. The authors wish to express their sincere thanks to M. Brecht Dirix and Mrs. Leentje Persoons for evaluation of the antiviral activities (Rega Institute, Leuven, Belgium).

CONFLICT OF INTERESTS

The authors declare that there are no conflicts of interest.

ORCID

Hassan B. Lazrek  <http://orcid.org/0000-0002-3849-9092>

REFERENCES

- [1] A. Jemal, R. Siegel, E. Ward, T. Murray, J. Xu, M. J. Thun, *CA Cancer J. Clin.* **2007**, *57*, 43.
- [2] R. Snoeck, G. Andrei, E. de Clercq, *Drugs* **1999**, *57*, 187.
- [3] Y.-N. Wen, Z.-F. Zhang, N.-N. Liu, G. Andrei, R. Snoeck, Y.-H. Xiang, D. Schols, X. Chen, Z.-Y. Zhang, Q.-S. J. M. C. Zhang, *Med. Chem.* **2017**, *13*, 453.
- [4] Z. Moussa, M. A. M. S. El-Sharief, S. Y. Abbas, *Eur. J. Med. Chem.* **2016**, *122*, 419.
- [5] C. B. Thompson, *Science* **1995**, *267*, 1456.
- [6] D. Leung, G. Abbenante, D. P. Fairlie, *J. Med. Chem.* **2000**, *43*, 305.
- [7] M. W. Boudreau, J. Peh, P. J. Hergenrother, *ACS Chem. Biol.* **2019**, *14*, 2335.
- [8] S. Storey, *Nat. Rev. Drug Discov.* **2008**, *7*, 971.
- [9] F. Nainu, A. Shiratsuchi, Y. Nakanishi, *Front. Immunol.* **2017**, *8*, 1220.
- [10] E. Brazeau, R. Mahalingam, D. Gilden, M. Wellish, B. B. Kaufer, N. Osterrieder, S. Pugazhenth, *J. Neurovirol.* **2010**, *16*, 133.
- [11] A. D. Badley, A. A. Pilon, A. Landay, D. H. Lynch, *Blood* **2000**, *96*, 2951.
- [12] C. M. Galmarini, J. R. Mackey, C. Dumontet, *Lancet Oncol.* **2002**, *3*, 415.
- [13] M. Ferrero, V. Gotor, *Chem. Rev.* **2000**, *100*, 4319.
- [14] R. C. Yang, H. Zhu, X. Y. Jin, Q. Xiao, Y. Ju, *Adv. Mat. Res.* **2014**, *881*, 405.
- [15] C. McGuigan, C. J. Yarnold, G. Jones, S. Velázquez, H. Barucki, A. Brancale, G. Andrei, R. Snoeck, E. de Clercq, J. Balzarini, *J. Med. Chem.* **1999**, *42*, 4479.
- [16] J. Balzarini, C. McGuigan, *J. Antimicrob. Chemother.* **2002**, *50*, 5.
- [17] Z. Jahnz-Wechmann, G. Framski, P. Januszczak, J. Boryski, *J. Med. Chem.* **2015**, *97*, 388.
- [18] C. McGuigan, H. Barucki, A. Carangio, S. Blewett, G. Andrei, R. Snoeck, E. de Clercq, J. Balzarini, J. T. Erichsen, *J. Med. Chem.* **2000**, *43*, 4993.
- [19] H. S. Pentikis, M. Matson, G. Atiee, B. Boehlecke, J. T. Hutchins, J. M. Patti, G. W. Henson, A. Morris, *Antimicrob. Agents Chemother.* **2011**, *55*, 2847.
- [20] T. Gregorić, M. Sedić, P. Grbčić, A. Tomljenović Paravić, S. Kraljević Pavelić, M. Cetina, R. Vianello, S. Raić-Malić, *Eur. J. Med. Chem.* **2017**, *125*, 1247.
- [21] M. Hossam, D. S. Lasheen, N. S. M. Ismail, A. Esmat, A. M. Mansour, A. N. B. Singab, K. A. M. Abouzid, *Eur. J. Med. Chem.* **2018**, *144*, 330.
- [22] C. S. de Oliveira, B. F. Lira, J. M. Barbosa-Filho, J. G. Lorenzo, P. F. de Athayde-Filho, *Molecules* **2012**, *17*, 10192.
- [23] S. S. De, M. P. Khambete, M. S. Degani, *Bioorg. Med. Chem. Lett.* **2019**, *29*, 1999.
- [24] N. M. Sankhe, E. Durgashivaprasad, N. Gopalan Kutty, J. Venkata Rao, K. Narayanan, N. Kumar, P. Jain, N. Udupa, P. Vasanth Raj, *Arab. J. Chem.* **2019**, *12*, 2548.
- [25] C. D., Mohan, N. C., Anilkumar, S., Rangappa, M. K., Shanmugam, S., Mishra, A., Chinnathambi, S. A., Alharbi, A., Bhattacharjee, G., Sethi, A. P., Kumar, Basappa, K. S., Rangappa, *Front. Oncol.* **2018**, *8*, 42.
- [26] A.-E. El Mansouri, M. Maatallah, H. Ait Benhassou, A. Moumen, A. Mehdi, R. Snoeck, G. Andrei, M. Zahouily, H. B. Lazrek, *Nucleosides Nucleotides Nucleic Acids* **2020**, *39*, 1088.
- [27] A.-e El Mansouri, A. Oubella, A. Mehdi, M. Y. Aitltto, M. Zahouily, H. Morjani, H. B. Lazrek, *Bioorg. Chem.* **2020**, *108*, 104558.
- [28] F. Gao, T. Wang, J. Xiao, G. Huang, *Eur. J. Med. Chem.* **2019**, *173*, 274.
- [29] R. Chinchilla, C. Najera, *Chem. Rev.* **2007**, *107*, 874.
- [30] Z. Janeba, A. Holý, R. Pohl, R. Snoeck, G. Andrei, E. de Clercq, J. Balzarini, *Can. J. Chem.* **2010**, *88*, 628.
- [31] R. Chinchilla, C. Najera, *Chem. Soc. Rev.* **2011**, *40*, 5084.
- [32] A. Behr, A. J. Vorholt, K. A. Ostrowski, T. Seidensticker, *Green Chem.* **2014**, *16*, 982.
- [33] M. J. Robins, P. J. Barr, *Tetrahedron Lett.* **1981**, *22*, 421.
- [34] Z. Janeba, J. Balzarini, G. Andrei, R. Snoeck, E. de Clercq, M. J. Robins, *J. Med. Chem.* **2005**, *48*, 4690.
- [35] M. J. Robins, I. Nowak, V. K. Rajwanshi, K. Miranda, J. F. Cannon, M. A. Peterson, G. Andrei, R. Snoeck, E. de Clercq, J. Balzarini, *J. Med. Chem.* **2007**, *50*, 3897.
- [36] R. Romeo, S. V. Giofre, A. Garozzo, B. Bisignano, A. Corsaro, M. A. Chiacchio, *Bioorg. Med. Chem.* **2013**, *21*, 5688.
- [37] A. Mieczkowski, E. Tomczyk, M. Makowska, A. Nasulewicz-Goldeman, R. Gajda, K. Woźniak, J. Wietrzyk, *Synthesis* **2015**, *48*, 566.
- [38] Z. Liu, D. Li, S. Li, D. Bai, X. He, Y. Hu, *Tetrahedron* **2007**, *63*, 1931.
- [39] N. Fresneau, M.-A. Hiebel, L. A. Agrofoglio, S. Berteina-Raboin, *Tetrahedron Lett.* **2012**, *53*, 1760.
- [40] X. Jiao, D. J. Kopecky, J. Liu, J. C. Jaen, M. G. Cardozo, R. Sharma, N. Walker, H. Wesche, S. Li, E. Farrelly, S. H. Xiao, Z. Wang, F. Kayser, *Bioorg. Med. Chem. Lett.* **2012**, *22*, 6212.
- [41] S. Bhilare, H. Shet, Y. S. Sanghvi, A. R. Kapdi, *Molecules* **2020**, *25*, 1645.
- [42] Y. Takita, K.-i Sano, K. Kurosaki, N. Kawata, H. Nishiguchi, M. Ito, T. Ishihara, *Appl. Catal., A* **1998**, *167*, 49.
- [43] A. El Maadi, J. Bennazha, J. M. Réau, A. Boukhari, E. M. Holt, *Mater. Res. Bull.* **2003**, *38*, 865.
- [44] K. Dānoun, Y. Essamlali, O. Amadine, R. Tabit, A. Fihri, C. Len, M. Zahouily, *Appl. Organomet. Chem.* **2018**, *32*, e4232.
- [45] A.-E. E. Mansouri, M. Zahouily, H. B. Lazrek, *Synth. Commun.* **2019**, *49*, 1802.
- [46] P. G. Anantharaju, B. D. Reddy, M. A. Padukudru, C. M. Kumari Chitturi, M. G. Vimalambike, S. V. Madhunapantula, *Cancer Biol. Ther.* **2017**, *18*, 492.
- [47] B. Winther, N. Mygind, *Inflammopharmacology* **2003**, *11*, 445.
- [48] N. Vale, A. Ferreira, J. Matos, P. Fresco, M. J. Gouveia, *Molecules* **2018**, *23*, 2318.
- [49] T. Constantinescu, C. N. Lungu, I. Lung, *Molecules* **2019**, *24*, 1505.
- [50] G. Toth, K. Mazak, S. Hosztafi, J. Kokosi, B. Noszal, *J. Pharm. Biomed. Anal.* **2013**, *76*, 112.

- [51] L. R. Jevric, M. Z. Karadzic, A. I. Mandic, S. O. Podunavac Kuzmanovic, S. Z. Kovacevic, A. R. Nikolic, A. M. Okljesa, M. N. Sakac, K. M. Penov Gasi, S. Z. Stojanovic, *J. Pharm. Biomed. Anal.* **2017**, 134, 27.
- [52] Z. Y. Wu, N. Liu, B. Qin, L. Huang, F. Yu, K. Qian, S. L. Morris-Natschke, S. Jiang, C. H. Chen, K. H. Lee, L. Xie, *ChemMedChem* **2014**, 9, 1546.
- [53] A. Vaidya, A. K. Jain, B. R. Prashantha Kumar, G. N. Sastry, S. K. Kashaw, R. K. Agrawal, *Arab. J. Chem.* **2017**, 10, S3936.
- [54] A.-E. El Mansouri, A. Oubella, M. Maatallah, M. Y. Aitltto, M. Zahouily, H. Morjani, H. B. Lazrek, *Bioorg. Med. Chem. Lett.* **2020**, 30, 127438.
- [55] M. Pandurangan, G. Enkhtaivan, D. H. Kim, *J. Mol. Recognit.* **2016**, 29, 426.
- [56] R. Mutazah, H. A. Hamid, A. N. Mazila Ramli, M. F. Fasihi Mohd Aluwi, M. M. Yusoff, *Food Chem. Toxicol.* **2020**, 135, 110869.
- [57] I. M. Abdel-Rahman, M. Mustafa, S. A. Mohamed, R. Yahia, M. Abdel-Aziz, G. E.-D. A. Abuo-Rahma, A. M. Hayallah, *Bioorg. Chem.* **2021**, 107, 104629.
- [58] G. M. Morris, R. Huey, W. Lindstrom, M. F. Sanner, R. K. Belew, D. S. Goodsell, A. J. Olson, *J. Comput. Chem.* **2009**, 30, 2785.
- [59] J. W. Becker, J. Rotonda, S. M. Soisson, R. Aspiotis, C. Bayly, S. Francoeur, M. Gallant, M. Garcia-Calvo, A. Giroux, E. Grimm, *J. Med. Chem.* **2004**, 47, 2466.
- [60] L. Baddi, D. Ouzebla, A.-E. El Mansouri, M. Smietana, J.-J. Vasseur, H. B. Lazrek, *Nucleosides Nucleotides Nucleic Acids* **2021**, 40, 43.

SUPPORTING INFORMATION

Additional Supporting Information may be found online in the supporting information tab for this article.

How to cite this article: A. El Mansouri, A. Oubella, K. Dânoun, M. Ahmad, J. Neyts, D. Jochmans, R. Snoeck, G. Andrei, H. Morjani, M. Zahouily, H. B. Lazrek, *Arch. Pharm.* **2021**, e2100146. <https://doi.org/10.1002/ardp.202100146>